

Article

Synthesis of Mono- and Polyazole Hybrids Based on Polyfluoroflavones

Mariya A. Panova, Konstantin V. Shcherbakov, Ekaterina F. Zhilina, Yanina V. Burgart and Victor I. Saloutin * 

Postovsky Institute of Organic Synthesis, Ural Branch of the Russian Academy of Sciences, 22/20 Kovalevskoy St, Yekaterinburg 620108, Russia

* Correspondence: victor.saloutin@yandex.ru or saloutin@ios.uran.ru

Abstract: The possibility of functionalization of 2-(polyfluorophenyl)-4*H*-chromen-4-ones, with them having different numbers of fluorine atoms, with 1,2,4-triazole or imidazole under conditions of base-promoted nucleophilic aromatic substitution has been shown. A high selectivity of mono-substitution was found with the use of an azole (1.5 equiv.)/NaOBu^t (1.5 equiv.)/MeCN system. The structural features of fluorinated mono(azoly)-substituted flavones in crystals were established using XRD analysis. The ability of penta- and tetrafluoroflavones to form persubstituted products with triazole under azole (6 equiv.)/NaOBu^t (6 equiv.)/DMF conditions was found in contrast to similar transformations with imidazole. On the basis of mono(azoly)-containing polyfluoroflavones in reactions with triazole and pyrazole, polynuclear hybrid compounds containing various azole fragments were obtained. For poly(pyrazolyl)-substituted flavones, green emission in the solid state under UV-irradiation was found, and for some derivatives, weak fungistatic activity was found.

Keywords: polyfluoroflavones; 1*H*-1,2,4-triazole; imidazole; nucleophilic aromatic substitution; regioselectivity; azoly-substituted flavones; photoluminescence



Citation: Panova, M.A.; Shcherbakov, K.V.; Zhilina, E.F.; Burgart, Y.V.; Saloutin, V.I. Synthesis of Mono- and Polyazole Hybrids Based on Polyfluoroflavones. *Molecules* **2023**, *28*, 869. <https://doi.org/10.3390/molecules28020869>

Academic Editor: Joseph Sloop

Received: 30 December 2022

Revised: 11 January 2023

Accepted: 11 January 2023

Published: 15 January 2023



Copyright: © 2023 by the authors. Licensee MDPI, Basel, Switzerland. This article is an open access article distributed under the terms and conditions of the Creative Commons Attribution (CC BY) license (<https://creativecommons.org/licenses/by/4.0/>).

1. Introduction

Flavones based on a 2-phenylchromen-4-one backbone are important heteroaromatic scaffolds in organic chemistry due to their availability and significant synthetic and biological potential [1–5]. The uniqueness of this heterocyclic backbone is also due to the fact that its derivatives are widely represented in the plant world, which often determines their diverse biological action [6–11]. Isolation, identification, and chemical modification of flavones of plant origin is one of the rapidly developing areas in drug design [12,13]. Another equally important area of progress in the chemistry of flavones is the development of synthetic strategies for their modification. In addition, here, certain successes have recently been achieved, for example, its modification has been proposed by the Buchwald–Hartwig reaction [14], metal-catalyzed cascade rearrangements [15,16], electrochemical dimerization [17], CH-functionalization [18], etc. However, all of these transformations most often require expensive catalysts or complex installations.

In turn, fluorinated flavones offer extra possibilities for their functionalization in reactions with nucleophilic reagents. Fluoroaromatic compounds are well known to be perspective frameworks for their modification by different methods for formation of new C–C and C–heteroatom bonds [19–21], including C–N bond formation in reactions with azole-type heterocycles [22–24]. There are known approaches to the synthesis of chromone–azole dyads [25]; however, data on direct functionalization of fluorine-containing flavones with azoles under S_NAr reaction conditions have only been only in publications from our research team [26,27], although the reaction of nucleophilic aromatic substitution of fluorine atoms is a quite simple, economically and environmentally friendly process, which offers the possibility of substitution for fluorinated substrates with advantages over reactions that use expensive catalysts [28]. To date, we have considerable practice in the

synthesis and modification of polyfluoroflavones [26,27,29–32]. Previously, we proposed a convenient and efficient method for the synthesis of B-ring polyfluorinated flavones (2-(polyfluorophenyl)chromen-4-ones) [29], which can be involved in S_NAr reactions to obtain polynuclear heterocyclic compounds based on flavones and azoles. We have shown the possibility of controlling the fluorine atoms substitution of 2-(polyfluorophenyl)chromen-4-ones by pyrazole and assumed the mechanism for sequential fluorine substitution on an example of 2-pentafluorophenyl-4*H*-chromen-4-one [26].

Within this work in continuation of our research in this area, the features of the functionalization of 2-(polyfluoroaryl)-4*H*-chromen-4-ones **1–3**, with them having different numbers of fluorine atoms in the aryl substituent (Figure 1), by 1*H*-1,2,4-triazole and imidazole under conditions of base-promoted nucleophilic aromatic substitution were studied.

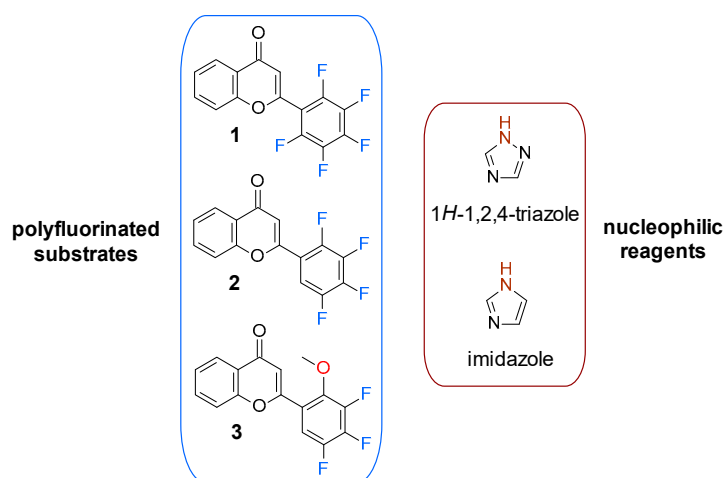


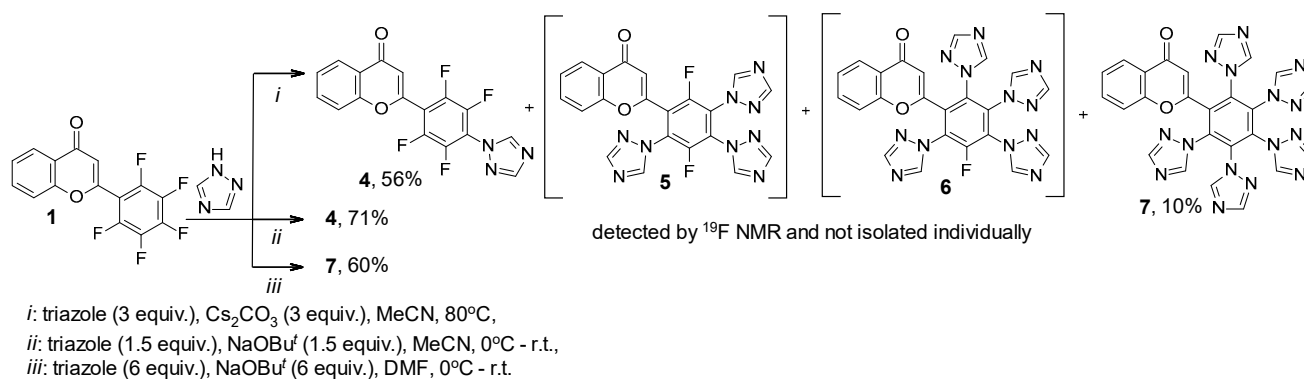
Figure 1. Polyfluorinated flavones in the S_NAr reaction with the 1*H*-1,2,4-triazole and imidazole under study in this work.

The introduction of azole fragments has a wide perspective due to their ability to form various noncovalent interactions with different therapeutic targets, which is valuable for drug design. Different azole derivatives have significant potential for medicinal chemistry [33–40]. Of particular interest are 1*H*-1,2,4-triazole and imidazole derivatives, which are known to possess therapeutic effect against drug-resistant pathogens [40–42]. The way to more effective medicines is through the synthesis of azole hybrids with other pharmacophores [27,43–45], which might be flavones, with them having a pyran framework that determines their great potential as antiviral antibacterial agents. Polyazole hybrid derivatives are also given special attention due to their potential applications as electron-transporting materials, emitters, and host materials in OLEDs, the most attractive products of organic electronics [46–48]. In this regard, the synthesis of hybrid compounds based on the flavone and azole cycles seems to be a prominent problem, which can be solved by the S_NAr reaction of polyfluorinated flavones with azoles.

2. Results

The study of the reaction of polyfluoroflavones **1–3** with 1*H*-1,2,4-triazole and imidazole under base-promoted nucleophilic aromatic substitution was carried out according to three synthetic protocols developed during the research of transformations with pyrazole [26]. The application of the Cs_2CO_3 -promoted conditions will allow for observation of the spectrum of possible substituted products, while the application of the $NaOBu^t$ -promoted conditions should facilitate for selective mono- and persubstitution of fluorine, which depends on variation of the nucleophile and base loading. The most convenient method for identifying fluorine-containing compounds in their mixtures is ^{19}F NMR spectroscopy data.

The reaction of flavone **1** with 3 equiv. of triazole and Cs_2CO_3 in MeCN led to a mono-, tri-, tetra-, and penta(1*H*-1,2,4-triazol-1-yl)-substituted products mixture, from which only mono- and penta-substituted flavones **4** and **7** were isolated by column chromatography (Scheme 1). The ^{19}F NMR data of fluorine-containing products **4**–**7** and their ratio in the reaction mixture are shown in Table 1. Under optimized conditions, selective synthesis of mono- and penta(1*H*-1,2,4-triazol-1-yl)-substituted products **4** and **7** with a good preparative yield was achieved (Scheme 1).



Scheme 1. Reaction of 2-(pentafluorophenyl)-4*H*-chromen-4-one **1** with 1*H*-1,2,4-triazole.

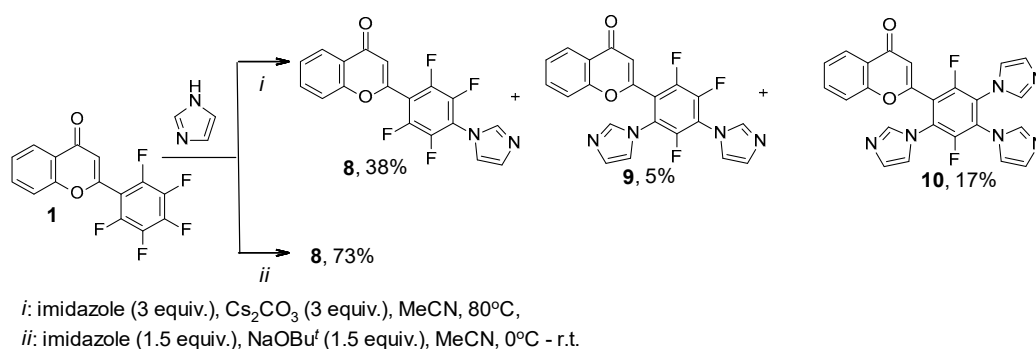
Table 1. ^{19}F NMR data of mixture of Cs_2CO_3 -promoted reaction of flavone **1** with 1*H*-1,2,4-triazole.

Compound	^{19}F NMR Data	
	δ , ppm	Products Ratio, %
4	16.66, m; 24.82, m	97
5	15.95, m; 26.03, m; 26.86, m	1
6	31.53, m	2

In contrast to the transformations with triazole, the reaction of flavone **1** with 3 equiv. of imidazole under the same conditions resulted in the formation of mono-, di-, and tri(1*H*-imidazol-1-yl)-substituted products **8**–**10**, which were isolated with a poor preparative yield. The ^{19}F NMR data of fluorine-containing products **8**–**10** and their ratio in the mixture are shown in Table 2. Under conditions preferable to monosubstitution, 2-[2,3,5,6-tetrafluoro-4-(1*H*-imidazol-1-yl)phenyl]-4*H*-chromen-4-one **8** was synthesized with a good yield (Scheme 2). In addition, under conditions conducive to the formation of a persubstituted product, the reaction of these reagents is extremely nonselective.

Table 2. ^{19}F NMR data of a mixture of Cs_2CO_3 -promoted reaction of flavone **1** with imidazole.

Compound	^{19}F NMR Data	
	δ , ppm, <i>J</i> , Hz	Products Ratio, %
8	14.88, m; 24.52, m	63
9	23.57, m; 26.31, m; 30.56, m	6
10	31.46, dm, <i>J</i> = 14.2 Hz; 41.17, dd, <i>J</i> = 14.9, 1.1 Hz	31



Scheme 2. Reaction of 2-(pentafluorophenyl)-4*H*-chromen-4-one **1** with imidazole.

It should be noted that for 2-[2,5-difluoro-3,4,6-tri(1*H*-imidazol-1-yl)phenyl]-4*H*-chromen-4-one **10**, an isomeric structure—2-[3,5-difluoro-2,4,6-tri(1*H*-imidazol-1-yl)phenyl]-substituted product can be proposed. The structures of **9** and **10** were solved on the basis of a comparative analysis of ¹H, ¹⁹F NMR data of these compounds **9** and **10**, and NMR data of formerly synthesized [26] tri(1*H*-pyrazol-1-yl)-substituted analogue **A** (Appendix A, Table A1).

The crystal structures of 2-[2,3,5,6-tetrafluoro-4-(1*H*-azol-1-yl)phenyl]-4*H*-chromen-4-ones flavones **4** and **8** were confirmed by XRD analysis (Figures 2 and 3). Both homologues **4** and **8** have similar structural characteristics, in contrast to the pyrazolyl-substituted analogue [26], which does not have intramolecular interactions coordinating both pyrone and aryl moieties, which are therefore aplanar. In addition, the introduction of triazole and imidazole fragments has a critical effect on the structure of their unit cell in the crystal. Thus, a cell of compound **4** has a rhombic syngony and compound **8** has a monoclinic syngony. It is important to note that for two systems of atoms C16C11C2C3 and C17N1C14C15 of product **4** and similar systems C3C2C11C12 and C13C14N1C17 of analogue **8**, the torsion angles have values close in absolute value, but pairwise opposite in sign, equal to 42.70(0.76), −47.50(0.85), and −58.89(0.31), 56.50(0.34) degrees for **4** and **8**, respectively. The unit cell of the crystal **4** consists of four molecules due to the formation of O⋯H, F⋯F, and C⋯C sp² short intermolecular contacts (O3⋯H17 2.373, O3⋯H18 2.634, C5⋯C14 3.331(8), C9⋯C12 3.303(7), F2⋯F4 2.889(5) Å) (Figure 2). The unit cell of crystal **8** also consists of four molecules stabilized by C⋯H, C⋯F, and C⋯C sp² short intermolecular contacts (C18⋯H5 2.80(2), C7⋯F3 3.117(3), C9⋯C16 3.396(3) Å) (Figure 3).

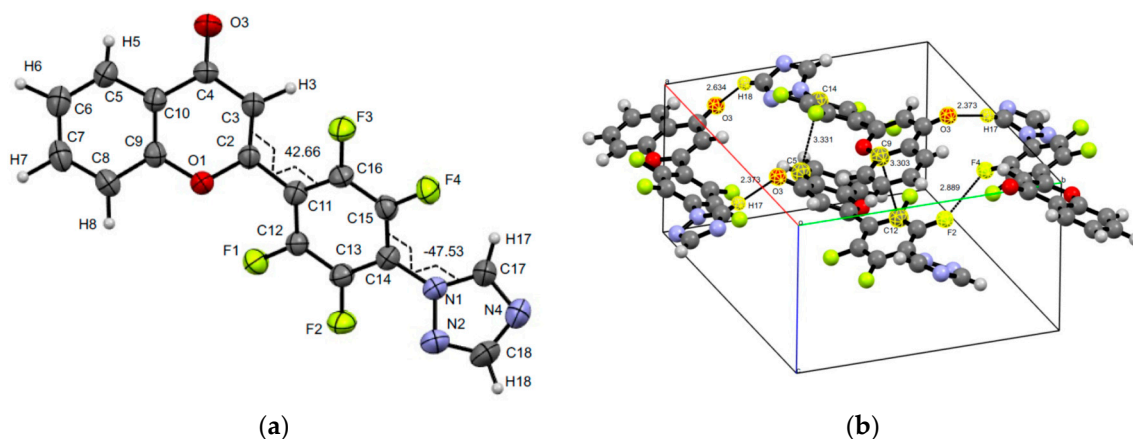


Figure 2. Molecular structure and selected torsions (a), and unit cell (b) of compound **4** with atoms represented as thermal ellipsoids of thermal vibrations with a 50% probability.

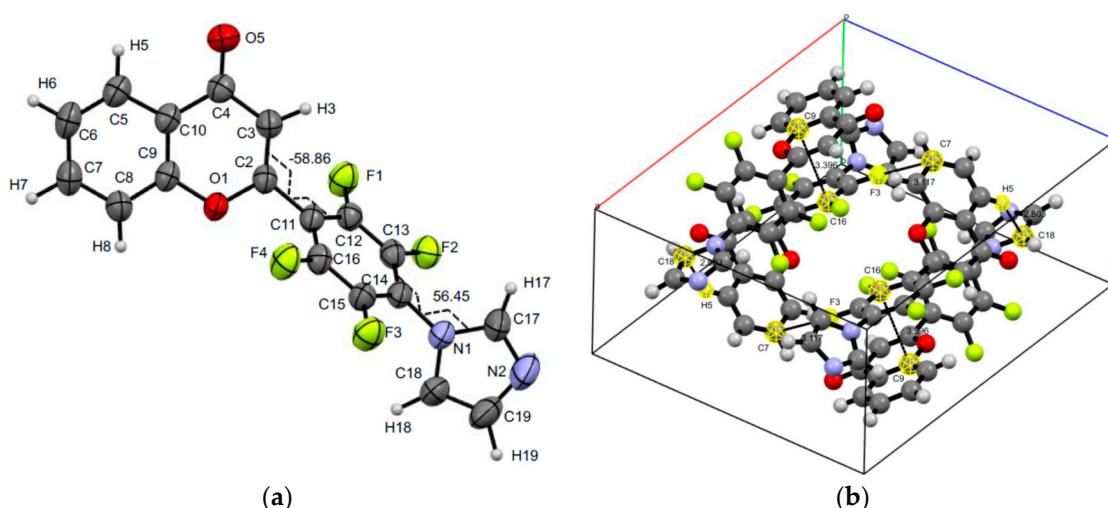
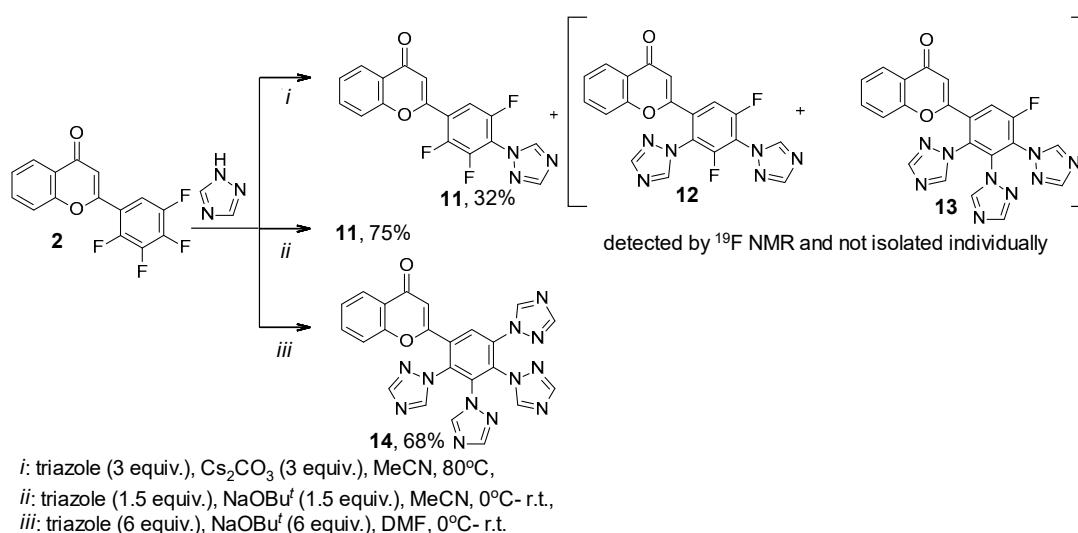
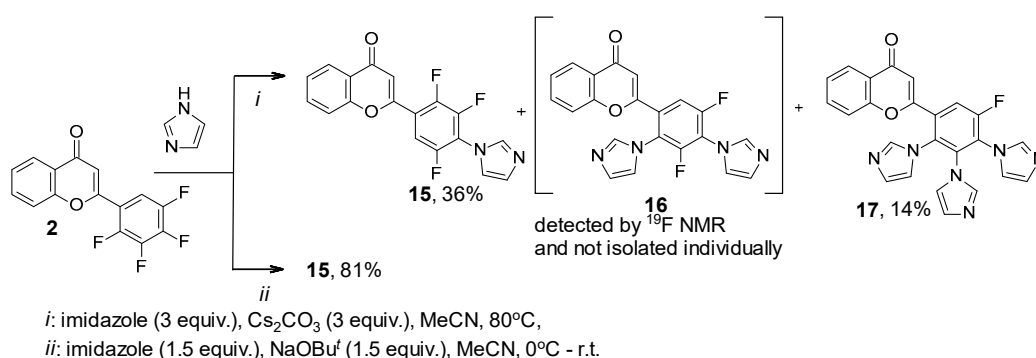


Figure 3. Molecular structure and selected torsions (a), and unit cell (b) of compound **8** with atoms represented as thermal ellipsoids of thermal vibrations with a 50% probability.

Furthermore, we introduced flavone **2**, with it having 2,3,4,5-tetrafluorophenyl substituent, in the S_NAr reaction with triazole and imidazole. The reaction of compound **2** with 3 equiv. of triazole (Scheme 3) and imidazole (Scheme 4) in the presence of Cs_2CO_3 in MeCN led to mono-, di-, and tri(azol-1-yl)-substituted products mixture **11–13** and **15–17**, respectively. The ^{19}F NMR data of fluorine-containing flavones **11–13** and **15–17** and their ratio in the mixture are shown in Table 3. Under optimized conditions, selective synthesis of mono- **11** and tetra(triazol-1-yl)-substituted products **14** was conducted with a good preparative yield (Scheme 3). However, under similar conditions, only mono(imidazolyl)-substituted flavone **15** was obtained in a good yield from the reaction with imidazole, and it was not possible to isolate the persubstituted product (Scheme 4) as in the reaction of flavone **1** (Scheme 2). This may indicate a lower reactivity of imidazole compared to triazole and the previously studied pyrazole under the conditions used [26].



Scheme 3. Reaction of 2-(2,3,4,5-tetrafluorophenyl)-4H-chromen-4-one **2** with 1H-1,2,4-triazole.



Scheme 4. Reaction of 2-(2,3,4,5-tetrafluorophenyl)-4H-chromen-4-one **2** with imidazole.

Table 3. ¹⁹F NMR data of mixtures of Cs₂CO₃-promoted reactions of flavone **2** with 1*H*-1,2,4-triazole and imidazole.

Compound	¹⁹ F NMR Data	
	δ, ppm	Products Ratio, %
11	23.72, d, <i>J</i> = 19.9 Hz; 24.92, ddd, <i>J</i> = 20.1, 14.7, 5.6 Hz; 39.24, dd, <i>J</i> = 14.1, 10.7 Hz	56
12	39.54, dd, <i>J</i> = 15.2, 9.8 Hz; 39.86, dd, <i>J</i> = 16.0, 5.7 Hz	34
13	49.03, d, <i>J</i> = 9.2 Hz	10
15	21.76, dd, <i>J</i> = 20.0, 1.9 Hz; 24.80, ddd, <i>J</i> = 20.1, 14.4, 6.1 Hz, 38.16, m	35
16	39.41, m; 39.71, m	20
17	47.34, d, <i>J</i> = 9.1 Hz	45

The structure of 2-[2,3,5-trifluoro-4-(1*H*-imidazol-1-yl)phenyl]-4H-chromen-4-one **15** was confirmed by XRD analysis (Figure 4). As well as products **4** and **8**, compound **15** has no intramolecular interactions, which coordinated both pyrone and aryl moieties. However, the replacement of fluorine at the C6' site by hydrogen allows the mutual position of these two moieties of flavone **15** in crystal close to coplanar. Torsions C3C2C11C12 and C1N1C14C13 are −7.10(0.30) and −48.14(0.27) degrees. The unit cell of the crystal **15** is monoclinic, consists of four molecules, stabilized by pairs of O⋯H, C⋯O short intermolecular contacts (O4⋯H17 2.33(3), C17⋯O4 3.148(3), and C2⋯O4 3.127(2) Å).

The reaction of 2-(3,4,5-trifluoro-2-methoxy-phenyl)-4H-chromen-4-one **3** with 3 equiv. of triazole in the presence of Cs₂CO₃ in MeCN led to the formation of mono- and di(1*H*-1,2,4-triazol-1-yl)-substituted products **18**, **19**, which were isolated from the mixture (Scheme 5). In the ¹⁹F NMR spectrum of the mixture, in addition to the signals corresponding to products **18** and **19**, two pairs of signals were recorded, presumably assigned by us to compounds **20** and **21** (Table 4). Due to the low intensity and insufficient resolution of these signals, the possibility of their detection is difficult. We believe that the formation of product **20** is possible due to the demethylation of flavone **18** under the reaction conditions used. The formed phenolic group in compound **20** can be in equilibrium between keto and enol forms, and keto form may undergo a nucleophilic addition reaction with triazole followed by aromatization to provide flavone **21**.

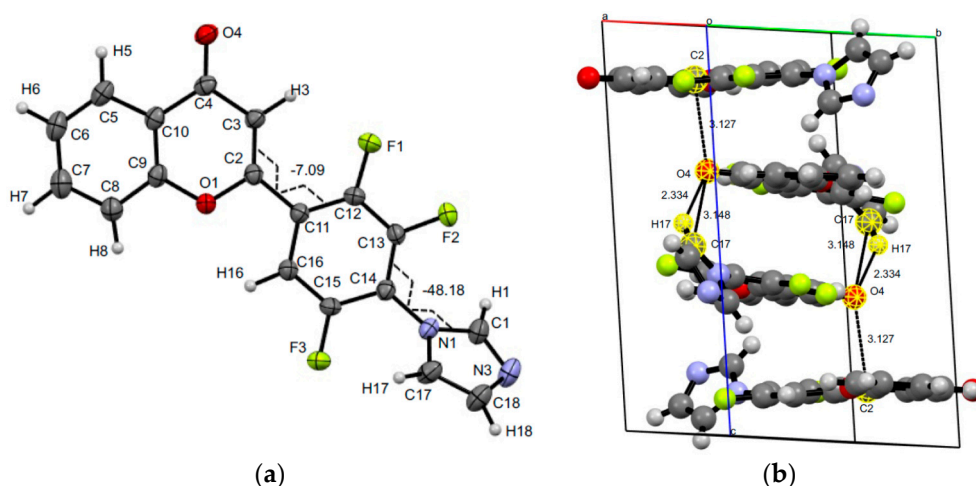
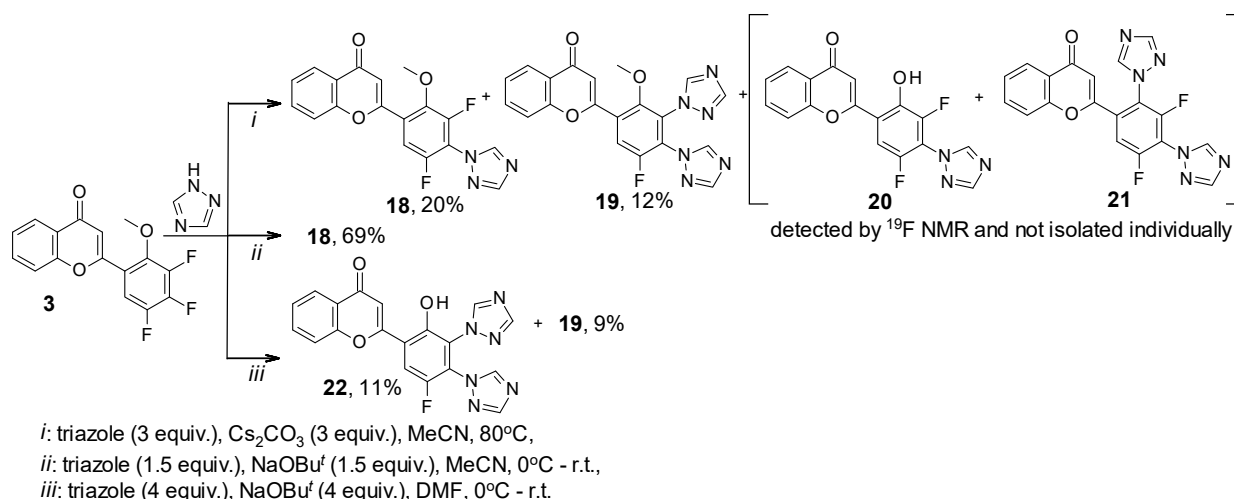


Figure 4. Molecular structure and selected torsions (a), and unit cell (b) of compound 15 with atoms represented as thermal ellipsoids of thermal vibrations with a 50% probability.



Scheme 5. Reaction of 2-(3,4,5-trifluoro-2-methoxyphenyl)-4H-chromen-4-one 3 with 1H-1,2,4-triazole.

Table 4. ^{19}F NMR data of mixture of Cs_2CO_3 -promoted reaction of flavone 3 and 1H-1,2,4-triazole.

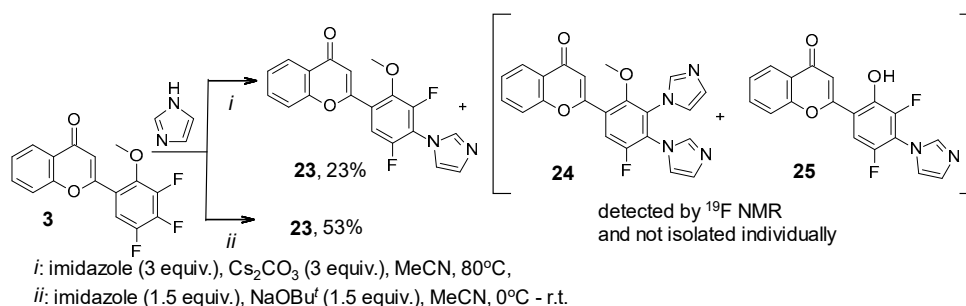
Compound	^{19}F NMR Data	
	δ , ppm	Products Ratio, %
18	29.29, m; 37.18, m	31
19	38.83, dd, $J = 9.9, 1.9$ Hz	64
20	38.77, m; 39.82, m	2
21	37.13, m; 39.63, m	3

Under NaOBu^t -promoted conditions for selective monosubstitution corresponding 2-[2,3,5,6-tetrafluoro-4-(1H-1,2,4-triazol-1-yl)phenyl]-4H-chromen-4-one 18 was synthesized with a good preparative yield. The reaction with four-fold excess of triazole and NaOBu^t led to flavone 19 and 2-[2-hydroxy-3,4-di(1H-1,2,4-triazol-1-yl)phenyl]-4H-chromen-4-one 22, which was obtained by demethylation of 2-methoxy-3,4-di(1H-1,2,4-triazol-1-yl)-substituted precursor 19, with poor yields, similar to pyrazolyl-substituted analogues [26]. The use of six-fold excess of triazole and NaOBu^t gave the same result as above with four-fold excess.

From the reaction of flavone **3** with 3 equiv. of imidazole in the presence of Cs_2CO_3 in MeCN, only mono-substituted product **23** was isolated individually. The ^{19}F NMR spectrum of the mixture (Table 5) also contained signals assigned to flavones **24** and **25** based on the conclusions given above for similar transformations with triazole. Under optimized conditions, 2-[3,5-difluoro-2-methoxy-4-(1*H*-imidazol-1-yl)phenyl]-4*H*-chromen-4-one **23** was synthesized (Scheme 6). Using an excess of this azole has not been successful in isolating any individual products.

Table 5. ^{19}F NMR data of mixture of Cs_2CO_3 -promoted reaction of flavone **3** and imidazole.

Compound	^{19}F NMR Data	
	δ , ppm	Products Ratio, %
23	27.60, m; 36.46, m	31
24	38.70, m	67
25	28.22, m; 38.63, m	2



Scheme 6. Reaction of 2-(3,4,5-trifluoro-2-methoxyphenyl)-4*H*-chromen-4-one **3** with imidazole.

The structures of 2-[5-fluoro-2-methoxy-3,4-di(1*H*-1,2,4-triazol-1-yl)phenyl]-4*H*-chromen-4-one **19** and 2-[4,5-difluoro-2-methoxy-4-(1*H*-1,2,4-imidazol-1-yl)phenyl]-4*H*-chromen-4-one **23** were confirmed by XRD analysis (Figures 5 and 6). Compounds **19** and **23** also do not have any intramolecular interactions. It was found that the introduction of one or two azole fragments affects the geometric parameters of crystals **19** and **23**. The unit cell of compound **19** has a triclinic syngony and consists of two molecules stabilized by a pair of short intramolecular contacts $\text{C} \cdots \text{F}$ ($\text{C10} \cdots \text{F1}$ 3.159(6) Å). The cell of compound **23** of the monoclinic system consists of four molecules forming short intermolecular contacts $\text{O} \cdots \text{H}$, $\text{C} \cdots \text{F}$ ($\text{O3} \cdots \text{H8}$ 2.568, $\text{O3} \cdots \text{H16}$ 2.32(3), $\text{C3} \cdots \text{F001}$ 3.148(3) Å). It should be noted that the torsion angles of two similar systems of atoms C16C11C2C3 and C3C2C11C12 of di(triazolyl)- and mono(imidazolyl)-substituted flavones **19** and **23** have a significant difference both in absolute value and in sign and are equal to $-22.81(0.72)$ and $8.64(0.33)$ degrees, respectively. The geometry of the azole fragments of molecules **19** and **23** does not reveal fundamental differences. The torsion angles of the atomic systems C18N1C15C16 , C20N4C14C15 , and C17N1C14C13 are $56.12(0.58)$, $56.96(3.50)$, and $49.82(0.37)$ degrees, respectively.

It should be noted that a common characteristic of the crystals of both mono(1*H*-imidazol-1-yl)-substituted products **15** and **23** is the formation of a unit cell of the monoclinic system. However, the torsion angles of the systems of atoms C3C2C11C12 , C1N1C14C13 of trifluoroflavone **15** and C3C2C11C12 and C17N1C14C13 of difluoroflavone **23** have practically equal absolute values and opposite values (Figures 4 and 6).

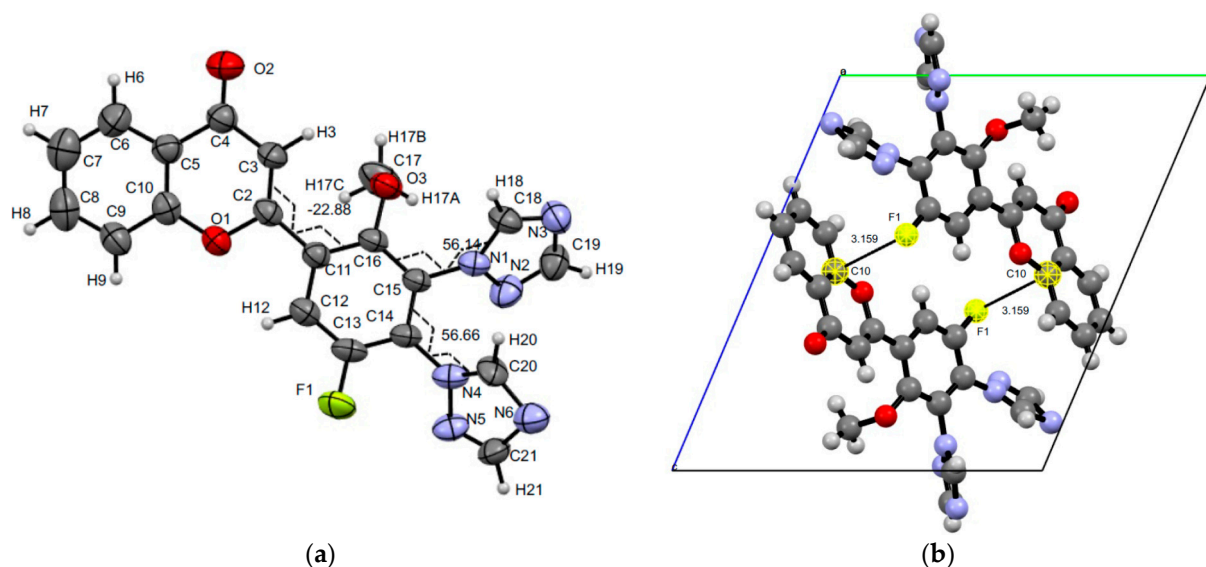


Figure 5. Molecular structure and selected torsions (a) and unit cell (b) of compound **19** with atoms represented as thermal ellipsoids of thermal vibrations with a 50% probability.

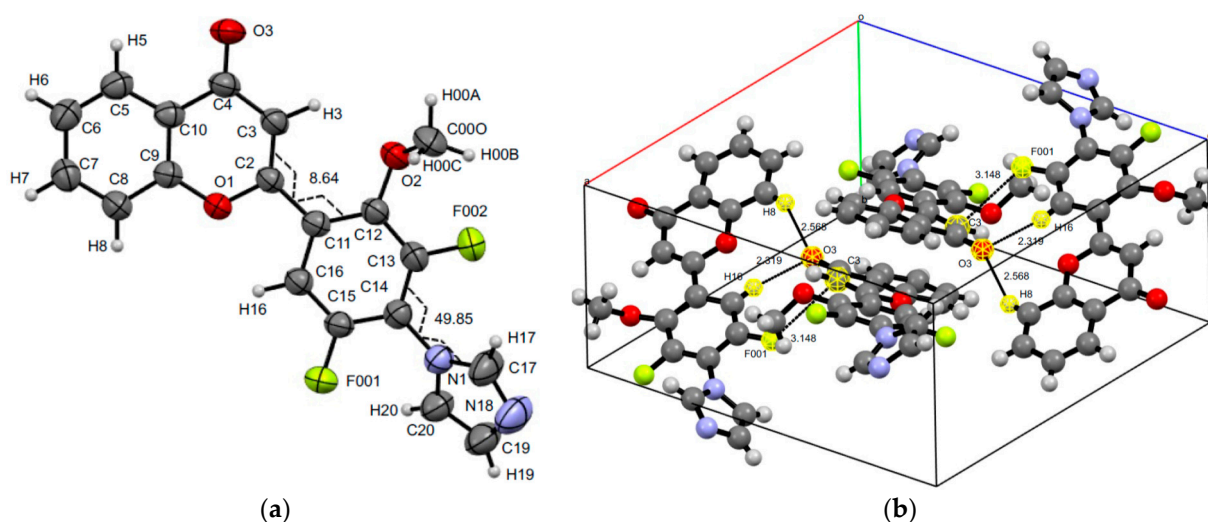
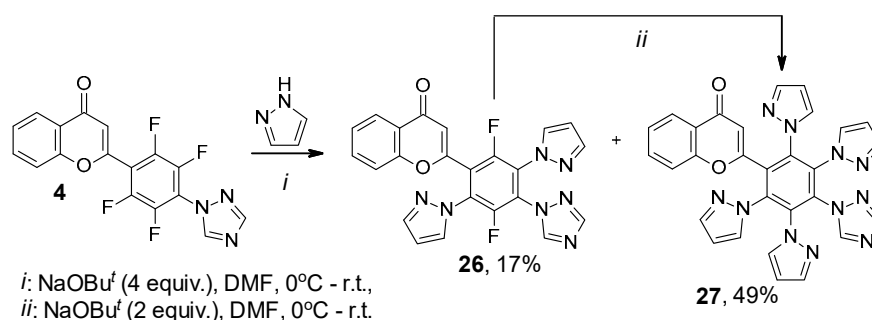


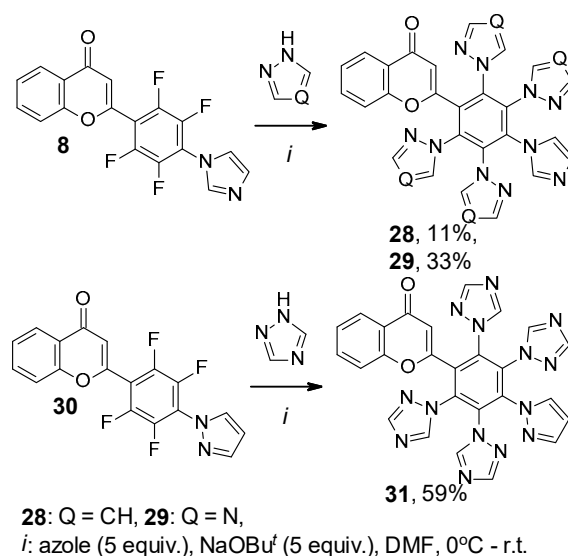
Figure 6. Molecular structure and selected torsions (a) and unit cell (b) of compound **23** with atoms represented as thermal ellipsoids of thermal vibrations with a 50% probability.

In this work, we also studied the possibility of the synthesis of 2-[poly(1*H*-azol-1-yl)phenyl]-4*H*-chromen-4-ones, involving two different azole-type heterocycles in their structure by the NaOBu^{*t*}-promoted S_NAr reaction of mono(1*H*-azol-1-yl)-substituted flavones with azoles.

Thus, the reaction of mono(triazolyl)-substituted flavone **4** with four-fold excess of pyrazole and NaOBu^{*t*} led to 2-[2,5-difluoro-3,6-di(1*H*-pyrazol-1-yl)-4-(1*H*-1,2,4-triazol-1-yl)phenyl]- and 2-[2,3,5,6-tetra(1*H*-pyrazol-1-yl)-4-(1*H*-1,2,4-triazol-1-yl)phenyl]-4*H*-chromen-4-ones **26** and **27**. Flavone **26** was shown to react with two-fold excess of pyrazole and NaOBu^{*t*} to form product of complete substitution **27** (Scheme 7). Under conditions preferable for persubstitution, flavone **8** reacts with pyrazole and triazole, leading to the formation of compounds **28** and **29**. Similarly, 2-(2,3,5,6-tetrafluoro-4-(1*H*-pyrazol-1-yl)phenyl)-4*H*-chromen-4-one **30** obtained earlier [26] forms product **31** with triazole (Scheme 8). Unfortunately, we have not yet succeeded in growing a suitable single crystal for XRD due to the limited solubility of polynuclear products **27–29** and **31** in organic solvents.



Scheme 7. Reaction of flavone 4 with pyrazole.



Scheme 8. Reaction of monoazoly-substituted flavone 4, 30 with azoles.

As is known, aryl-azole scaffolds are considered as promising materials for OLEDs [46–49]; therefore, we recorded the photoluminescence spectra for poly(azoly)-substituted flavones **28–31** and formerly synthesized penta(pyrazoly)-substituted analogue **32** [26]. It was found that 2-[4-(imidazoly)-2,3,5,6-tetra(pyrazoly)- and penta(pyrazoly)-substituted flavones **28** and **32** exhibit emission in the solid state under UV-irradiation, in contrast to poly(triazoly)-containing derivatives **29** and **31**. The emission spectra of these compounds were recorded, and the data are presented in Table 6 and Figure 7. Flavones **28** and **32** possess green emission with maxima 504 nm. The commission international de L'Eclairage (CIE) coordinates were (0.255; 0.528) and (0.255; 0.526) for **28** and **32**, respectively. Substitution of pyrazole fragment at C4' by imidazole results in a 1.6-fold increase in quantum yield (0.18 and 0.29 for **28** and **32**, correspondingly). Detailed data of the fluorescence lifetime measurements of flavones **28** and **32** are given in Appendix B.

Table 6. Photoluminescent data for compounds **28** and **32** in powder at r.t.

Compound	Emission, λ_{em} , nm	τ_{avg} , [ns]/ χ^2	Φ_F
28	504	7.72/ 1.109	0.29
32	504	6.81/ 1.206	0.18

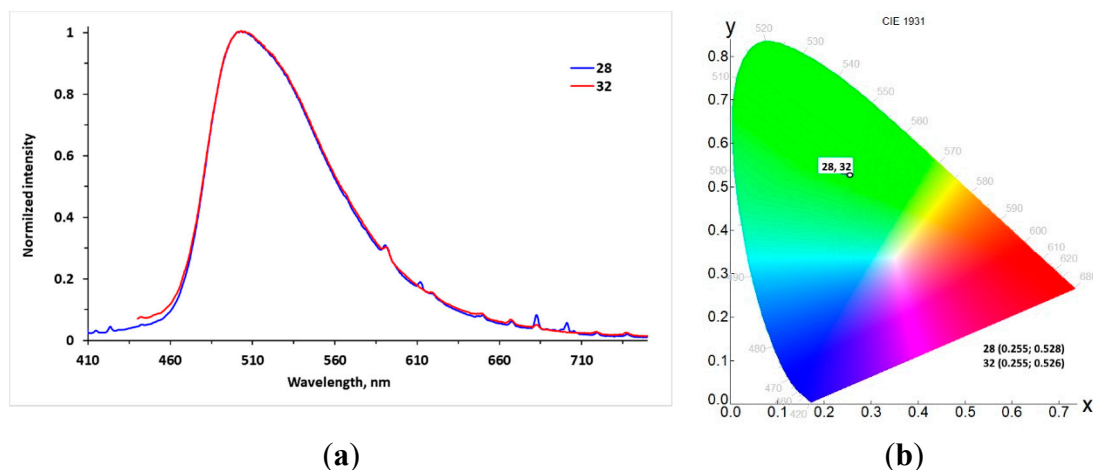


Figure 7. Emission (–) spectra (a) and CIE 1931 chromaticity diagram (b) for chromophores 28 and 32 in solid state.

Azoly-substituted flavones are of great interest in the search for the bioactive compounds among them, and, in particular, for antimycotic agents [50]; therefore, we screened the fungistatic activity of a number of compounds (Appendix C) obtained in this work and earlier [29] in relation to four control strains of clinically significant species of pathogenic fungi *Trichophyton rubrum*, *Epidermophyton floccosum*, *Microsporum canis*, and *Candida parapsilosis*. It was found that flavones **8** and **14** have a weak inhibitory effect against *T. rubrum* and *M. canis* (MIC 100 mg/mL), and derivatives **23** and **33**, combined methoxy and azole substituents, in the absence of fungistatic activity (MIC > 100 µg/mL) showed high and moderate activity in inhibiting the growth of 50% fungal culture (MIC₅₀ 1.56–12.5 µg/mL).

3. Materials and Methods

3.1. Chemistry: General Information and Synthetic Techniques

Solvents and reagents except fluorine-containing flavones are commercially available and were used without purification. The NMR spectra of the synthesized compounds (see Supplementary Materials) were recorded on Bruker DRX-400 and Bruker AVANCE III 500 spectrometers (¹H, 400.13 (DRX400) and 500.13 (AV500) MHz, ¹³C, 125.76 MHz, Me₄Si as an internal standard, ¹⁹F, 376.44 (DRX400) and 470.52 (AV500) MHz, C₆F₆ as an internal standard, chemical shifts were not converted to CCl₃F). IR spectra were recorded on a Perkin Elmer Spectrum Two FT-IR spectrometer (UATR) in the range of 4000–400 cm^{−1}. Elemental (C, H, N) analysis was performed on a Perkin Elmer PE 2400 Series II CHNS-O EA 1108 elemental analyzer. The melting points were measured on a Stuart SMP3 in open capillaries. The reaction progress was monitored by TLC on ALUGRAM Xtra SIL G/UV₂₅₄ sheets. The starting flavones (**1–3**) were synthesized by a procedure [29].

Synthetic technique A for the synthesis of azoly-substituted flavones using Cs₂CO₃. flavone (0.5 or 1 mmol), azole (3 equiv.), and Cs₂CO₃ (3 equiv.) were suspended in 10 mL of MeCN. The reaction mixture was heated to 80 °C. The reaction progress was monitored by TLC. At the end of the reaction, the mixture was diluted with water (10 mL) and extracted with CHCl₃ or DCM (2 × 10 mL). Organic layers were combined, and the solvent was removed. The residue was immobilized on silica gel and purified by column chromatography using an appropriate eluent mixture (2:1 v/v).

Synthetic technique B for the synthesis of azoly-substituted flavones using NaOBu^t. flavone (0.5 or 1 mmol) was dissolved in dry DMF (5 mL), placed in a sealed vial and cooled to 0 °C. Azole (from 1.5 to 6 equiv.) and NaOBu^t (from 1.5 to 6 equiv.) were suspended in dry DMF (5 mL) and stirred at room temperature for 5 min. The mixture was cooled to 0 °C and was added to a flavone solution in DMF while stirring. After 10 min. in a cooling bath (0 °C), the vial was removed and the reaction continued at room temperature. The

reaction progress was monitored by TLC. At the end, the reaction mixture was diluted with water (10 mL), stirred, and cooled. The formed precipitate was filtered off and washed with water. The water solution was neutralized with 0.1M HCl and extracted with CHCl₃ or DCM. The organic layer was separated, and the solvent was removed. Organic residues were combined, immobilized on silica gel and purified by column chromatography using an appropriate eluent mixture (2:1 *v/v*).

3.2. Spectral and Elemental Analysis Data of Synthesized Compounds

2-[2,3,5,6-Tetrafluoro-4-(1*H*-1,2,4-triazol-1-yl)phenyl]-4*H*-chromen-4-one (4). Yield 202 mg (56% according to technique A), 256 mg (71% according to technique B); white powder; mp 192–194 °C; IR ν 3108, 3043 (C–H^{Ar}), 1639 (C=O), 1528, 1485, 1381 (C=C^{Ar}, C–H^{Ar}, C–N), 1139, 1110 (C–F) cm^{−1}; ¹H NMR (500.13 MHz, CDCl₃) δ 6.68 (s, 1H, CH^{Pyranone}), 7.50 (m, 1H, CH^{Ar}), 7.53 (d, *J* = 8.6 Hz, 1H, CH^{Ar}), 7.76 (ddd, *J* = 8.6, 7.1, 1.7 Hz, 1H, CH^{Ar}), 8.26 (dd, *J* = 8.0, 1.5 Hz, 1H, CH^{Ar}), 8.29 (s, 1H, CH^{Triazole}), 8.52 (s, 1H, CH^{Triazole}) ppm; ¹³C NMR (125.76 MHz, CDCl₃) δ 113.7 (t, *J* = 15 Hz, C^{Ar}), 116.1 (t, *J* = 3 Hz, C^{Ar}), 118.2 (s, C^{Ar}), 118.8 (s, C^{Ar}), 123.9 (s, C^{Pyranone}), 125.9 (s, C^{Ar}), 126.0 (s, C^{Ar}), 134.5 (s, C^{Ar}), 141.7 (m, 2C^{ArF}), 144.7 (ddt, *J* = 257, 14, 5 Hz, 2C^{ArF}), 145.3 (t, *J* = 3 Hz, C^{Triazole}), 151.7 (s, C^{Ar}), 153.5 (s, C^{Triazole}), 156.6 (s, C^{Pyranone}), 177.0 (s, C^{Pyranone}) ppm; ¹⁹F NMR (470.52 MHz, CDCl₃) δ 16.66 (m, 2F), 24.83 (m, 2F) ppm; Anal. calcd. for C₁₇H₇F₄N₃O₂: C 56.52, H 1.95, N 11.63, found: C 56.26, H 1.84, N 11.38.

2-[2,3,4,5,6-Penta(1*H*-1,2,4-triazol-1-yl)phenyl]-4*H*-chromen-4-one (7). Yield 39 mg (7% according to technique A), 335 mg (60% according to technique B); light-yellow powder; mp 322–323 °C; IR ν 3118, 3086 (C–H^{Ar}), 1651 (C=O), 1514, 1459, 1379, 1272 (C=C^{Ar}, C–H^{Ar}, C–N) cm^{−1}; ¹H NMR (500.13 MHz, CDCl₃) δ 6.20 (s, 1H, CH^{Pyranone}), 7.16 (d, *J* = 8.4 Hz, 1H, CH^{Ar}), 7.42 (m, 1H, CH^{Ar}), 7.65 (ddd, *J* = 8.5, 7.2, 1.7 Hz, 1H, CH^{Ar}), 7.87 (s, 1H, CH^{Triazole}), 7.88 (s, 2H, CH^{Triazole}), 7.90 (s, 2H, CH^{Triazole}), 8.08 (dd, *J* = 8, 1.6 Hz, 1H, CH^{Ar}), 8.10 (s, 1H, CH^{Triazole}), 8.15 (s, 2H, CH^{Triazole}), 8.22 (s, 2H, CH^{Triazole}) ppm; ¹³C NMR (125.76 MHz, CDCl₃) δ 114.9, 117.4 (s, 2C^{Ar}), 123.2, 126.1, 126.5, 133.1, 134.3 (s, 2C^{Ar}), 134.9, 135.3, 136.1, 145.3 (s, 2C^{Triazole}), 145.7, 146.0 (s, 2C^{Triazole}), 153.4, 153.7 (s, 2C^{Triazole}), 153.7 (s, 2C^{Triazole}), 155.7, 175.8 ppm; Anal. Calcd. For C₂₅H₁₅N₁₅O₂: C 53.86, 2.71, N 37.69, found: C 53.60, H 2.68, N 37.69.

2-[2,3,5,6-Tetrafluoro-4-(1*H*-imidazol-1-yl)phenyl]-4*H*-chromen-4-one (8). Yield 137 mg (38% according to technique A), 263 mg (73% according to technique B); white powder, mp 172–174 °C; IR ν 3110 (C–H^{Ar}), 1653 (C=O), 1489, 1459, 1376 (C=C^{Ar}, C–H^{Ar}, C–N), 1224 (C–F) cm^{−1}; ¹H NMR (400.13 MHz, CDCl₃) δ 6.67 (s, 1H, CH^{Pyranone}), 7.31 (br.s., 1H, CH^{Imidazole}), 7.33 (br.s., 1H, CH^{Imidazole}), 7.48–7.53 (m, 2H, 2CH^{Ar}), 7.76 (ddd, *J* = 8.6, 7.3, 1.5 Hz, 1H, CH^{Ar}), 7.88 (br.s., 1H, CH^{Imidazole}), 8.27 (dd, *J* = 7.9, 1.5 Hz, 1H, CH^{Ar}) ppm; ¹³C NMR (125.76 MHz, CDCl₃) δ 112.0 (t, *J* = 15 Hz, C^{Ar}), 115.9 (t, *J* = 3 Hz, C^{Ar}), 118.2, 119.3 (t, *J* = 13 Hz, C^{Ar}), 119.7 (t, *J* = 2 Hz, C^{Imidazole}), 123.9, 125.9, 126.0, 130.6, 134.5, 137.5 (t, *J* = 4 Hz, C^{Imidazole}), 140.1–142.3 (m, 2C^{ArF}), 144.9 (ddt, *J* = 257, 14, 5 Hz, 2C^{ArF}), 152.0, 156.6, 177.1 ppm; ¹⁹F NMR (376.44 MHz, CDCl₃) δ 14.88 (dq, *J* = 6.0, 4.4, 2.4 Hz, 2F), 24.51 (dq, *J* = 7.3, 4.2 Hz, 2F) ppm; Anal. calcd. for C₁₈H₈F₄N₂O₂: C 60.01, H 2.24, N 7.78, found: C 59.89, H 2.30, N 7.96.

2-[2,3,5-Trifluoro-4,6-di(1*H*-imidazol-1-yl)phenyl]-4*H*-chromen-4-one (9). Yield 20 mg (5%); light-yellow powder, mp 200–203 °C; ¹H NMR (400.13 MHz, CDCl₃) δ 6.52 (d, *J* = 1.5 Hz, 1H, CH^{Pyranone}), 7.05 (br.s., 1H, CH^{Imidazole}), 7.13 (br.s., 1H, CH^{Imidazole}), 7.18 (d, *J* = 8.4 Hz, 1H, CH^{Ar}), 7.33 (br.s., 1H, CH^{Imidazole}), 7.35 (br.s., 1H, CH^{Imidazole}), 7.41–7.45 (m, 1H, CH^{Ar}), 7.65 (br.s., 1H, CH^{Imidazole}), 7.65 (dd, *J* = 15.7, 1.7 Hz, 1H, CH^{Ar}), 7.90 (br.s., 1H, CH^{Imidazole}), 8.17 (dd, *J* = 7.9, 1.5 Hz, 1H, CH^{Ar}) ppm; ¹⁹F NMR (376.44 MHz, CDCl₃) δ 23.60 (d, *J* = 22.2 Hz, 1F), 26.33 (ddd, *J* = 22.6, 13.0, 1.3 Hz, 1F), 30.57 (d, *J* = 13.0 Hz, 1F) ppm. Anal. calcd. for C₂₁H₁₁F₃N₄O₂: C 61.77, H 2.72, N 13.72, found: C 61.89, H 2.79, N 13.66.

2-[2,5-Difluoro-3,4,6-tri(1*H*-imidazol-1-yl)phenyl]-4*H*-chromen-4-one (10). Yield 95 mg (17%); light-yellow powder; mp 227–228 °C; ¹H NMR (400.13 MHz, CDCl₃) δ 6.51 (d, *J* = 1.3 Hz, 1H, CH^{Pyranone}), 6.81 (d, *J* = 1.3 Hz, 1H, CH^{Imidazole}), 6.83 (d, *J* = 1.2 Hz, 1H,

CH^{Imidazole}), 7.10 (d, $J = 1.2$ Hz, 1H, CH^{Imidazole}), 7.15–7.20 (m, 1H, CH^{Ar}), 7.21–7.23 (m, 3H, 3CH^{Imidazole}), 7.43–7.47 (m, 1H, CH^{Ar}), 7.50 (br.s, 2H, 2CH^{Imidazole}), 7.65–7.69 (m, 1H, CH^{Ar}), 7.70 (br.s, 1H, 1CH^{Imidazole}), 8.18 (dd, $J = 8.0, 1.6$ Hz, 1H, CH^{Ar}) ppm; ¹³C NMR (125.76 MHz, CDCl₃) δ 115.8 (d, $J = 3$ Hz, CH^{Pyranone}), 117.8, 119.0, 119.2, 120.0, 120.5 (d, $J = 17$ Hz, C^{ArF}), 123.3 (d, $J = 16$ Hz, C^{ArF}), 123.6, 125.6 (dd, $J = 15, 2$ Hz, C^{ArF}), 125.8–126.0 (m, C^{ArF}), 125.9, 126.2, 131.0, 131.46, 131.47, 134.7, 136.9 (d, $J = 3$ Hz, C^{ArF}), 137.0 (d, $J = 2$ Hz, C^{Imidazole}), 137.5 (d, $J = 2$ Hz, C^{Imidazole}), 148.3 (dd, $J = 256, 4$ Hz, C^{ArF}), 150.9 (dd, $J = 257, 4$ Hz, C^{ArF}), 152.7 (d, $J = 2$ Hz, C^{Imidazole}), 156.2, 176.6 ppm; ¹⁹F NMR (376.44 MHz, CDCl₃) δ 31.47 (dm, $J = 14.4$ Hz, 1F), 41.18 (dd, $J = 14.7, 1.2$ Hz, 1F) ppm. Anal. calcd. for C₂₄H₁₄F₂N₆O₂: C 63.16, H 3.09, N 18.41, found: C 62.90, H 2.82, N 18.24.

2-[2,3,5-Trifluoro-4-(1H-1,2,4-triazol-1-yl)phenyl]-4H-chromen-4-one (11). Yield 257 mg (75%); white powder; mp 210–211 °C; IR ν 3138, 3118, 3070 (C–H^{Ar}), 1634 (C=O), 1531, 1462, 1369 (C=C^{Ar}, C–H^{Ar}, C–N), 1040 (C–F) cm^{−1}; ¹H NMR (500.13 MHz, CDCl₃) δ 7.02 (s, 1H, CH^{Pyranone}), 7.49 (t, $J = 7.5$ Hz, 1H, CH^{Ar}), 7.58 (d, $J = 8.4$ Hz, 1H, CH^{Ar}), 7.74–7.79 (m, 2H, 2CH^{Ar}), 8.25 (dd, $J = 8.0, 1.6$ Hz, 1H, CH^{Ar}), 8.27 (s, 1H, CH^{Triazole}), 8.49 (s, 1H, CH^{Triazole}) ppm; ¹³C NMR (125.76 MHz, CDCl₃) δ 110.6 (dd, $J = 24, 4$ Hz, C^{Ar}), 113.9, 114.0, 118.0 (m, C^{Ar}, C^{Triazole}), 122.7 (t, $J = 9$ Hz, C^{Ar}), 123.8, 125.9, 134.5, 144.8–145.1 (m, C^{ArF}), 145.3 (t, $J = 3$ Hz, C^{Triazole}), 146.9–147.2 (m, C^{ArF}), 151.7 (ddd, $J = 254, 3, 2$ Hz, C^{ArF}), 153.3, 154.9 (td, $J = 4, 2$ Hz, C^{Pyranone}), 156.1, 177.6 ppm; ¹⁹F NMR (470.52 MHz, CDCl₃) δ 23.72 (d, $J = 20.1$ Hz, 1F), 24.92 (ddd, $J = 20.3, 14.5, 5.9$ Hz, 1F), 39.24 (dd, $J = 14.6, 10.8$ Hz, 1F) ppm; Anal. calcd. for C₁₇H₈F₃N₃O₂: C 59.48, H 2.35, N 12.24, found: C 54.40, H 2.32, N 12.29.

2-[2,3,4,5-Tetra(1H-1,2,4-triazol-1-yl)phenyl]-4H-chromen-4-one (14). Yield 333 mg (68%); light-yellow powder; mp 295–296 °C; IR ν 3134, 3108 (C–H^{Ar}), 1644 (C=O), 1508, 1467 (C=C^{Ar}, C–H^{Ar}, C–N) cm^{−1}; ¹H NMR (500.13 MHz, (CD₃)₂SO) δ 6.87 (s, 1H, CH^{Pyranone}), 7.22 (d, $J = 8.3$ Hz, 1H, CH^{Ar}), 7.49–7.53 (m, 1H, CH^{Ar}), 7.80 (ddd, $J = 8.7, 7.4, 1.6$ Hz, 1H, CH^{Ar}), 8.00 (s, 1H, CH^{Triazole}), 8.03 (dd, $J = 7.9, 1.5$ Hz, 1H, CH^{Ar}), 8.05 (s, 1H, CH^{Triazole}), 8.10 (s, 1H, CH^{Triazole}), 8.17 (s, 1H, CH^{Triazole}), 8.61 (s, 1H, CH^{Triazole}), 8.68 (s, 1H, CH^{Triazole}), 8.86 (s, 1H, CH^{Triazole}), 8.87 (s, 1H, CH^{Triazole}), 9.04 (s, 1H, CH^{Triazole}) ppm; ¹³C NMR (125.76 MHz, CDCl₃) δ 112.8, 118.1 (s, 2C^{Ar}), 122.9, 124.9, 126.1, 129.3, 131.1, 132.9 (d, $J = 2$ Hz, C^{Ar}), 133.6, 134.9, 135.2, 146.0, 146.8, 146.9, 147.2, 152.6, 152.7, 152.8, 153.1, 155.4, 158.6, 176.5 ppm; Anal. calcd. for C₂₃H₁₄N₁₂O₂: C 56.33, H 2.88, N 34.27, found: C 56.11, H 2.90, N 34.22.

2-[2,3,5-Trifluoro-4-(1H-imidazol-1-yl)phenyl]-4H-chromen-4-one (15). Yield 277 mg (81%); white powder; mp 204–206 °C; IR ν 3160, 3133, 3077 (C–H^{Ar}), 1625, 1606 (C=O), 1515, 1465, 1351 (C=C^{Ar}, C–H^{Ar}, C–N), 1007 (C–F) cm^{−1}; ¹H NMR (500.13 MHz, CDCl₃) δ 7.00 (s, 1H, CH^{Pyranone}), 7.31 (br.s., 2H, 2CH^{Imidazole}), 7.47–7.50 (m, 1H, 1CH^{Ar}), 7.58 (d, $J = 8.2$ Hz, 1H, CH^{Ar}), 7.71–7.74 (m, 1H, 1CH^{Ar}), 7.75–7.78 (m, 1H, 1CH^{Ar}), 7.88 (br.s., 1H, CH^{Imidazole}), 8.25 (dd, $J = 8.0, 1.6$ Hz, 1H, CH^{Ar}) ppm; ¹³C NMR (125.76 MHz, CDCl₃) δ 110.6 (dd, $J = 25, 4$ Hz, C^{Ar}), 113.5, 113.6, 118.0, 118.5 (dd, $J = 17, 12$ Hz, C^{ArF}), 119.8 (t, $J = 2$ Hz, C^{Imidazole}), 120.7 (t, $J = 9$ Hz, C^{ArF}), 123.7, 125.9, 130.2, 134.4, 137.6 (t, $J = 4$ Hz, C^{Imidazole}), 145.3 (ddd, $J = 256, 17, 4$ Hz, C^{ArF}), 146.2 (ddd, $J = 258, 14, 4$ Hz, C^{ArF}), 151.2 (dt, $J = 251, 3$ Hz, C^{ArF}), 155.1 (m, C^{ArF}), 156.1, 177.7 ppm; ¹⁹F NMR (470.52 MHz, CDCl₃) δ 21.78 (dd, $J = 19.8, 1.2$ Hz, 1F), 24.83 (ddd, $J = 20.1, 14.3, 1.2$ Hz, 1F), 38.13–38.18 (m, 1F) ppm; Anal. calcd. for C₁₈H₉F₃N₂O₂: C 63.16, H 2.65, N 8.18, found: C 63.16, H 2.81, N 8.29.

2-[5-Fluoro-2,3,4-tri(1H-imidazol-1-yl)phenyl]-4H-chromen-4-one (17). Yield 31 mg (14%); yellow powder; mp 168–170 °C; ¹H NMR (400.13 MHz, CDCl₃) δ 6.40 (s, 1H, CH^{Pyranone}), 6.57 (t, $J = 1.3$ Hz, 1H, CH^{Imidazole}), 6.73 (d, $J = 1.1$ Hz, 1H, CH^{Ar}), 6.78 (t, $J = 1.3$ Hz, 1H, CH^{Imidazole}), 7.03–7.04 (m, 2H, CH^{Imidazole}), 7.13 (br.s, 1H, CH^{Imidazole}), 7.15–7.17 (m, 2H, CH^{Imidazole}), 7.39 (br.s, 1H, CH^{Imidazole}), 7.40–7.44 (m, 1H, CH^{Ar}), 7.47 (br.s, 1H, CH^{Imidazole}), 7.65 (ddd, $J = 8.7, 7.3, 1.6$ Hz, 1H, CH^{Ar}), 7.85 (d, $J = 9.1$ Hz, 1H, CH^{Ar}), 8.15 (dd, $J = 8.0, 1.5$ Hz, 1H, CH^{Ar}) ppm; ¹³C NMR (125.76 MHz, CDCl₃) δ 112.8, 117.9, 118.5 (d, $J = 23$ Hz, C^{ArF}), 119.0, 119.1, 120.0, 123.4, 125.7–125.8 (m, C^{ArF}, C^{Ar}), 126.1, 129.6 (d, $J = 4$ Hz, C^{ArF}), 131.0, 131.1, 131.5, 132.8 (d, $J = 2$ Hz, C^{ArF}), 132.9 (d, $J = 9$ Hz, C^{ArF}), 134.7, 136.5, 137.0 (d, $J = 2$ Hz, C^{Imidazole}), 137.4, 155.9, 156.2 (d, $J = 259$ Hz, C^{ArF}), 158.6

(d, $J = 2$ Hz, C^{Pyranone}), 177.1 ppm; ¹⁹F NMR (376.44 MHz, CDCl₃) δ 47.37 (d, $J = 9.2$ Hz, 1F) ppm; Anal. calcd. for C₂₄H₁₅FN₆O₂: C 65.75, H 3.45, N 19.17, found: C 65.95, H 3.32, N 18.84.

2-[3,5-Difluoro-4-(1H-1,2,4-triazol-1-yl)-2-methoxyphenyl]-4H-chromen-4-one (**18**). Yield 35 mg (20% according to technique A), 123 mg (69% according to technique B); white powder; mp 172–174 °C; IR ν 3143, 3108, 3063 (C–H^{Ar}, C–H^{Alk}), 1665 (C=O), 1523, 1464, 1377 (C=C^{Ar}, C–H^{Ar}, C–N), 1034 (C–F) cm^{−1}; ¹H NMR (400.13 MHz, CDCl₃) δ 4.06 (d, $J = 1.9$ Hz, 3H, OCH₃), 7.15 (s, 1H, CH^{Pyranone}), 7.45–7.49 (m, 1H, CH^{Ar}), 7.56 (dd, $J = 8.4$, 0.5 Hz, CH^{Ar}), 7.66 (dd, $J = 10.4$, 2.3 Hz, CH^{Ar}), 7.75 (ddd, $J = 8.7$, 7.2, 1.7 Hz, CH^{Ar}), 8.25 (s, 1H, CH^{Triazole}), 8.26 (dd, $J = 7.9$, 1.6 Hz, CH^{Ar}), 8.45 (br.s, 1H, CH^{Triazole}) ppm; ¹³C NMR (125.76 MHz, CDCl₃) δ 62.1 (d, $J = 6$ Hz, C^{OMe}), 111.2 (dd, $J = 23$, 4 Hz, C^{ArF}), 113.6, 117.6 (dd, $J = 16$, 14 Hz, C^{ArF}), 118.0, 123.8, 125.6, 125.8, 127.3 (dd, $J = 9$, 4 Hz, C^{ArF}), 134.2, 144.0 (dd, $J = 12$, 4 Hz, C^{ArF}), 145.4 (br.s, C^{Triazole}), 150.5 (dd, $J = 257$, 4 Hz, C^{ArF}), 151.4 (dd, $J = 252$, 3 Hz, C^{ArF}), 153.1, 156.2, 157.2 (dd, $J = 4$, 2 Hz, C^{Pyranone}), 178.2 ppm; ¹⁹F NMR (376.44 MHz, CDCl₃) δ 29.29–29.30 (m, 1F), 37.19 (dd, $J = 10.5$, 1.3 Hz, 1F) ppm; Anal. calcd. for C₁₈H₁₁F₂N₃O₃: C 60.85, H 3.12, N 11.83, found: C 60.92, H 3.26, N 11.72.

2-[5-Fluoro-2-methoxy-3,4-di(1H-1,2,4-triazol-1-yl)phenyl]-4H-chromen-4-one (**19**). Yield 24 mg (12%); white powder; mp 203–204 °C; IR ν 3113, 3100, 2953, 2924 (C–H^{Ar}, C–H^{Alk}), 1640 (C=O), 1510, 1467, 1374 (C=C^{Ar}, C–H^{Ar}, C–N), 1008 (C–F) cm^{−1}; ¹H NMR (400.13 MHz, CDCl₃) δ 3.49 (s, 3H, OCH₃), 7.16 (s, 1H, CH^{Pyranone}), 7.48–7.52 (m, 1H, CH^{Ar}), 7.59 (d, $J = 8.4$ Hz, 1H, CH^{Ar}), 7.76–7.80 (m, 1H, CH^{Ar}), 7.96–8.01 (m, 3H, CH^{Triazole}), 8.27 (dd, $J = 8.0$, 1.4 Hz, 1H, CH^{Ar}), 8.37 (d, $J = 1.5$ Hz, 1H, CH^{Ar}), 8.42 (s, 1H, CH^{Triazole}) ppm; ¹³C NMR (125.76 MHz, CDCl₃) δ 62.4 (s, C^{OMe}), 113.4, 118.0 (d, $J = 24$ Hz, C^{ArF}), 118.0, 123.8, 124.9 (d, $J = 15$ Hz, C^{ArF}), 125.9, 126.0, 129.0 (d, $J = 8$ Hz, C^{ArF}), 129.6 (d, $J = 2$ Hz, C^{Triazole}), 134.5, 145.7 (d, $J = 2$ Hz, C^{Triazole}), 146.3, 151.0 (d, $J = 4$ Hz, C^{ArF}), 152.6 (d, $J = 253$ Hz, C^{ArF}), 152.8, 152.9, 156.3, 157.1 (d, $J = 2$ Hz, C^{Pyranone}), 177.9 ppm; ¹⁹F NMR (376.44 MHz, CDCl₃) δ 38.81 (dd, $J = 9.9$, 1.6 Hz, 1F) ppm; Anal. calcd. for C₂₀H₁₃FN₆O₃: C 59.41, H 3.24, N 20.78, found: C 59.51, H 3.23, N 20.79.

2-[5-Fluoro-2-hydroxy-3,4-di(1H-1,2,4-triazol-1-yl)phenyl]-4H-chromen-4-one (**22**). Yield 22 mg (11%); yellow powder; mp 313–316 °C; ¹H NMR (400.13 MHz, (CD₃)₂SO) δ 7.04 (s, 1H, CH^{Pyranone}), 7.52–7.56 (m, 1H, CH^{Ar}), 7.78–7.80 (m, 1H, CH^{Ar}), 7.88 (ddd, $J = 8.6$, 7.2, 1.6 Hz, 1H, CH^{Ar}), 8.07 (s, 1H, CH^{Triazole}), 8.09 (dd, $J = 8.1$, 1.5 Hz, 1H, CH^{Ar}), 8.11 (s, 1H, CH^{Triazole}), 8.26 (d, $J = 10.4$ Hz, 1H, CH^{Ar}), 8.76 (s, 1H, CH^{Triazole}), 8.79 (s, 1H, CH^{Triazole}), 10.98 (s, 1H, OH) ppm; ¹³C NMR (125.76 MHz, (CD₃)₂SO) δ 112.6, 118.3 (d, $J = 23$ Hz, C^{ArF}), 118.7, 123.3 (d, $J = 9$ Hz, C^{ArF}), 124.0, 124.7, 124.8 (d, $J = 15$ Hz, C^{ArF}), 125.7, 134.5, 146.6, 147.3, 148.7 (d, $J = 2$ Hz, C^{Triazole}), 149.1 (d, $J = 244$ Hz, C^{ArF}), 152.3, 152.5, 156.0, 159.0, 177.1 ppm; ¹⁹F NMR (376.44 MHz, (CD₃)₂SO) δ 30.74 (d, $J = 9.6$ Hz, 1F) ppm.

2-[3,5-Difluoro-4-(1H-imidazol-1-yl)-2-methoxyphenyl]-4H-chromen-4-one (**23**). Yield 39 mg (23% according to technique A), 94 mg (53% according to technique B); white powder; mp 176–177 °C; IR ν 3108, 3043, 2999, 2950 (OMe, C–H^{Ar}), 1630 (C=O), 1524, 1480, 1370 (C=C^{Ar}, C–H^{Ar}, C–O, C–N), 1112 (C–F) cm^{−1}; ¹H NMR (400.13 MHz, CDCl₃) δ 4.04 (d, $J = 1.7$ Hz, 3H, OMe), 7.14 (s, 1H, CH^{Pyranone}), 7.27–7.29 (m, 2H, 2CH^{Imidazole}), 7.45–7.49 (m, 1H, 1CH^{Ar}), 7.55–7.57 (m, 1H, 1CH^{Ar}), 7.64 (dd, $J = 10.8$, 2.2 Hz, 1H, CH^{Ar}), 7.75 (ddd, $J = 8.6$, 7.2, 1.7 Hz, 1H, CH^{Ar}), 7.83 (br.s., 1H, CH^{Imidazole}), 8.25 (dd, $J = 8.0$, 1.5 Hz, 1H, CH^{Ar}) ppm; ¹³C NMR (125.76 MHz, CDCl₃) δ 62.1 (d, $J = 6$ Hz, C^{OMe}), 111.2 (dd, $J = 24$, 4 Hz, C^{Ar}), 113.3, 118.0, 118.2 (dd, $J = 14$, 2 Hz, C^{Ar}), 120.0 (t, $J = 2$ Hz, C^{Imidazole}), 123.8, 125.5–125.6 (m, C^{Ar}, C^{Imidazole}), 125.8, 129.9, 134.2, 137.7 (t, $J = 3$ Hz, C^{Imidazole}), 144.2 (dd, $J = 12$, 4 Hz, C^{Ar}), 150.1 (dd, $J = 254$, 4 Hz, C^{ArF}), 151.1 (dd, $J = 249$, 4 Hz, C^{ArF}), 156.2, 157.4 (dd, $J = 4$, 2 Hz, C^{Pyranone}), 178.2 ppm; ¹⁹F NMR (376.44 MHz, CDCl₃) δ 27.59–27.60 (m, 1F), 36.45–36.48 (m, 1F) ppm; Anal. calcd. for C₁₉H₁₂F₂N₂O₃: C 64.41, H 3.41, N 7.91, found: C 64.37, H 3.40, N 8.02.

2-[2,5-Difluoro-3,6-di(1H-pyrazol-1-yl)-4-(1H-1,2,4-triazol-1-yl)phenyl]-4H-chromen-4-one (**26**). Yield 39 mg (17%); white powder; mp 256–258 °C; IR ν 3130, 3106, 3071 (C–H^{Ar}), 1642 (C=O), 1529, 1483, 1390 (C=C^{Ar}, C–H^{Ar}, C–N), 1139, 1127 (C–F) cm^{−1}; ¹H NMR

(400.13 MHz, CDCl₃) δ 6.44 (d, J = 1.2 Hz, 1H, C^{Pyranone}), 6.45–6.46 (m, 1H, CH^{Imidazole}), 6.48–6.49 (m, 1H, CH^{Imidazole}), 7.19–7.21 (m, 1H, CH^{Ar}), 7.40–7.44 (m, 1H, CH^{Ar}), 7.58 (d, J = 1.6 Hz, 1H, C^{Ar}), 7.63–7.66 (m, 3H, CH^{Imidazole}), 7.84 (t, J = 2.6 Hz, 1H, C^{Imidazole}), 8.05 (s, 1H, CH^{Triazole}), 8.19 (dd, J = 8.0, 1.5 Hz, 1H, C^{Ar}), 8.24 (s, 1H, CH^{Triazole}) ppm; ¹³C NMR (125.76 MHz, CDCl₃) δ 108.4, 108.6, 115.0 (d, J = 3 Hz, C^{Pyrazole}), 118.0, 121.4 (d, J = 17 Hz, C^{ArF}), 123.7, 125.5 (dd, J = 14, 3 Hz, C^{ArF}), 125.6, 125.8, 126.3 (d, J = 17 Hz, C^{ArF}), 128.7 (dd, J = 14, 3 Hz, C^{ArF}), 132.0 (d, J = 4 Hz, C^{Pyrazole}), 132.3 (d, J = 2 Hz, C^{Pyrazole}), 134.1, 142.7, 142.9, 145.7 (d, J = 1 Hz, C^{Pyranone}), 148.0 (dd, J = 258, 4 Hz, C^{ArF}), 151.1 (dd, J = 257, 4 Hz, C^{ArF}), 153.1, 154.3 (d, J = 2 Hz, C^{Pyranone}), 177.2 ppm; ¹⁹F NMR (376.44 MHz, CDCl₃) δ 30.62 (dd, J = 14.4, 1.8 Hz, 1F), 30.75–39.80 (m, 1F) ppm; Anal. calcd. for C₂₃H₁₃F₂N₇O₂: C 60.40, 2.86, N 21.44, found: C 60.15, H 2.68, N 21.54.

2-[2,3,5,6-Tetra(1H-pyrazol-1-yl)-4-(1H-1,2,4-triazol-1-yl)phenyl]-4H-chromen-4-one (27). Yield 136 mg (49%); yellow powder; mp 299–301 °C; IR ν 3126, 3092 (C–H^{Ar}), 1646 (C=O), 1525, 1468, 1389 (C=C^{Ar}, C–H^{Ar}, C–N) cm^{−1}; ¹H NMR (400.13 MHz, CDCl₃) δ 5.30 (s, 1H, CH^{Pyrazole}), 6.08 (s, 1H, CH^{Pyrazole}), 6.16–6.18 (m, 5H, CH^{Pyranone}, CH^{Pyrazole}), 7.11 (d, J = 8.4 Hz, 1H, CH^{Ar}), 7.24 (d, J = 2.5 Hz, 1H, CH^{Pyrazole}), 7.29 (d, J = 2.5 Hz, 1H, CH^{Pyrazole}), 7.32–7.36 (m, 1H, CH^{Ar}), 7.43 (d, J = 1.6 Hz, 2H, CH^{Pyrazole}), 7.49 (d, J = 1.6 Hz, 2H, CH^{Pyrazole}), 7.54–7.59 (m, 1H, CH^{Ar}), 7.74 (s, 1H, CH^{Triazole}), 8.05 (s, 1H, CH^{Triazole}), 8.06–8.08 (m, 1H, CH^{Ar}) ppm; ¹³C NMR (125.76 MHz, CDCl₃) δ 108.0 (s, 2C^{Pyrazole}), 108.2 (s, 2C^{Pyrazole}), 113.3, 117.8, 123.3, 125.4, 125.7 (s, 2C^{Ar}), 131.8 (s, 2C^{Pyrazole}), 132.1 (s, 2C^{Pyrazole}), 132.7, 133.8 (s, 2C^{Ar}), 135.2, 135.9, 138.2, 142.2 (s, 2C^{Pyrazole}), 142.3 (s, 2C^{Pyrazole}), 145.9, 152.3, 156.0, 156.6, 177.0 ppm; Anal. calcd. for C₂₉H₁₉N₁₁O₂: C 62.92, 3.46, N 27.83, found: C 63.15, H 3.68, N 27.69.

2-[4-(1H-Imidazol-1-yl)-2,3,5,6-tetra(1H-pyrazol-1-yl)phenyl]-4H-chromen-4-one (28). Yield 31 mg (11%); yellow powder; mp 320–321 °C; IR ν 3127 (C–H^{Ar}), 1649 (C=O), 1525, 1467, 1388 (C=C^{Ar}, C–H^{Ar}, C–N) cm^{−1}; ¹H NMR (400.13 MHz, CDCl₃) δ 6.03 (s, 1H, CH^{Pyranone}), 6.12–6.13 (m, 1H, CH^{Pyrazole}), 6.15 (dd, J = 4.3, 2.2 Hz, 4H, CH^{Pyrazole}), 7.11 (d, J = 8.3 Hz, 1H, CH^{Ar}), 7.20–7.23 (m, 3H, CH^{Pyrazole}, CH^{Imidazole}), 7.31–7.34 (m, 3H, CH^{Ar}, CH^{Pyrazole}, CH^{Imidazole}), 7.39 (d, J = 1.6 Hz, 2H, CH^{Pyrazole}), 7.41 (d, J = 1.6 Hz, 1H, CH^{Imidazole}), 7.47 (d, J = 1.5 Hz, 2H, CH^{Pyrazole}), 7.55 (ddd, J = 8.6, 7.3, 1.6 Hz, 1H, CH^{Ar}), 8.06 (dd, J = 7.9, 1.5 Hz, 1H, CH^{Ar}) ppm; ¹³C NMR (125.76 MHz, CDCl₃) δ 107.3, 107.5 (s, 2C^{Pyrazole}), 107.8 (s, 2C^{Pyrazole}), 113.2, 117.9, 123.3, 125.3, 125.6, 131.5, 131.9 (s, 2C^{Ar}), 132.0 (s, 2C^{Pyrazole}), 132.2 (s, 2C^{Pyrazole}), 133.7, 135.8, 138.3, 138.4, 141.7 (s, 2C^{Ar}), 141.7 (s, 2C^{Pyrazole}), 141.9 (s, 2C^{Pyrazole}), 156.0, 157.1, 177.1 ppm; Anal. calcd. for C₃₀H₂₀N₁₀O₂: C 65.21, 3.65, N 25.35, found: C 65.15, H 3.57, N 25.55.

2-[4-(1H-Imidazol-1-yl)-2,3,5,6-tetra(1H-1,2,4-triazol-1-yl)phenyl]-4H-chromen-4-one (29). Yield 92 mg (33%); pale pink powder; mp 299–301 °C; IR ν 3123, 3105 (C–H^{Ar}), 1647 (C=O), 1510, 1464, 1378 (C=C^{Ar}, C–H^{Ar}, C–N) cm^{−1}; ¹H NMR (500.13 MHz, (CD₃)₂SO) δ 6.30 (s, 1H, CH^{Pyranone}), 6.84 (s, 1H, CH^{Imidazole}), 7.01 (t, J = 1.3 Hz, 1H, CH^{Imidazole}), 7.34 (d, J = 8.2 Hz, 1H, CH^{Ar}), 7.47–7.49 (m, 1H, CH^{Ar}), 7.52 (s, 1H, CH^{Imidazole}), 7.80 (ddd, J = 8.7, 7.2, 1.7 Hz, 1H, CH^{Ar}), 7.92 (dd, J = 8.0, 1.6 Hz, 1H, CH^{Ar}), 8.08 (s, 2H, CH^{Triazole}), 8.11 (s, 2H, CH^{Triazole}), 8.63 (s, 2H, CH^{Triazole}), 8.82 (s, 2H, CH^{Triazole}) ppm; ¹³C NMR (125.76 MHz, CDCl₃) δ 113.7, 117.9, 121.0, 122.4, 124.9, 126.3, 129.3, 130.6, 134.0 (s, 2C^{Ar}), 135.0, 135.5 (s, 2C^{Ar}), 136.0, 137.9, 146.7 (s, 2C^{Triazole}), 146.8 (s, 2C^{Triazole}), 152.9 (s, 2C^{Triazole}), 152.9 (s, 2C^{Triazole}), 154.8, 155.4, 175.4 ppm; Anal. calcd. for C₂₆H₁₆N₁₄O₂: C 56.11, 2.90, N 35.24, found: C 56.30, H 2.98, N 35.04.

2-[4-(1H-Pyrazol-1-yl)-2,3,5,6-tetra(1H-1,2,4-triazol-1-yl)phenyl]-4H-chromen-4-one (31). Yield 159 mg (59%); pale pink powder; mp 309–310 °C; IR ν 3113 (C–H^{Ar}), 1651 (C=O), 1511, 1466, 1386 (C=C^{Ar}, C–H^{Ar}, C–N) cm^{−1}; ¹H NMR (500.13 MHz, (CD₃)₂SO) δ 6.31–6.32 (m, 1H, CH^{Pyrazole}), 6.32 (s, 1H, CH^{Pyranone}), 7.34 (d, J = 8.2 Hz, 1H, CH^{Ar}), 7.46–7.49 (m, 1H, CH^{Ar}), 7.56 (d, J = 1.7 Hz, 1H, CH^{Pyrazole}), 7.67 (d, J = 2.5 Hz, 1H, CH^{Pyrazole}), 7.79 (ddd, J = 8.7, 7.2, 1.7 Hz, 1H, CH^{Ar}), 7.92 (dd, J = 8.0, 1.6 Hz, 1H, CH^{Ar}), 8.04 (s, 2H, CH^{Triazole}), 8.05 (s, 2H, CH^{Triazole}), 8.53 (s, 2H, CH^{Triazole}), 8.82 (s, 2H, CH^{Triazole}) ppm; ¹³C NMR (125.76 MHz, (CD₃)₂SO) δ 107.9, 113.7, 118.0, 122.4, 124.9, 126.3, 130.8, 133.1, 133.9 (s, 2C^{Ar}), 135.1,

135.4 (s, 2C^{Ar}), 137.6, 142.5, 146.8 (s, 2C^{Triazole}), 146.9 (s, 2C^{Triazole}), 152.7 (s, 2C^{Triazole}), 152.9 (s, 2C^{Triazole}), 155.0, 155.4, 175.5 ppm; Anal. calcd. for C₂₆H₁₆N₄O₂: C 56.11, 2.90, N 35.24, found: C 56.26, H 2.99, N 35.11.

3.3. XRD Experiments

The X-ray studies were performed on an Xcalibur 3 CCD (Oxford Diffraction Ltd., Abingdon, UK) diffractometer with a graphite monochromator, $\lambda(\text{MoK}\alpha)$ 0.71073 Å radiation and T 295(2) K. An empirical absorption correction was applied. Using Olex2 [51], the structure was solved with the Superflip [52] structure solution program using charge flipping and refined with the ShelXL [53] refinement package using Least Squares minimization. All non-hydrogen atoms were refined in the anisotropic approximation; H-atoms at the C–H bonds were refined in the “rider” model with dependent displacement parameters. An empirical absorption correction was carried out through spherical harmonics, implemented in the SCALE3 ABSPACK scaling algorithm by the program “CrysAlisPro” (Rigaku Oxford Diffraction).

The main crystallographic data for **4**: C₁₇H₇F₄N₃O₂, *M* 361.26, orthorhombic, *a* 15.8944(12), *b* 12.7694(11), *c* 7.3245(6) Å, *V* 1486.6(2) Å³, space group Pna2₁, *Z* 4, $\mu(\text{Mo K}\alpha)$ 0.125 mm^{−1}, 256 refinement parameters, 3609 reflections measured, and 2493 unique (*R*_{int} = 0.0617), which were used in all calculations. CCDC 2225826 contains the supplementary crystallographic data for this compound.

The main crystallographic data for **8**: C₁₈H₈F₄N₂O₂, *M* 360.26, monoclinic, *a* 15.0164(11), *b* 7.9494(7), *c* 12.8592(10) Å, β 99.256(7)°, *V* 1515.0(2) Å³, space group P2₁/c, *Z* 4, $\mu(\text{Mo K}\alpha)$ 0.125 mm^{−1}, 268 refinement parameters, 4162 reflections measured, and 2246 unique (*R*_{int} = 0.0633), which were used in all calculations. CCDC 2,225,827 contains the supplementary crystallographic data for this compound.

The main crystallographic data for **15**: C₁₈H₉F₃N₂O₂, *M* 342.27, monoclinic, *a* 13.3565(10), *b* 7.8477(5), *c* 14.7075(12) Å, β 113.251(9)°, *V* 1416.4(2) Å³, space group P2₁/n, *Z* 4, $\mu(\text{Mo K}\alpha)$ 0.125 mm^{−1}, 262 refinement parameters, 3865 reflections measured, and 2692 unique (*R*_{int} = 0.0597), which were used in all calculations. CCDC 2,225,828 contains the supplementary crystallographic data for this compound.

The main crystallographic data for **19**: C₂₀H₁₃FN₆O₃, *M* 404.36, triclinic, *a* 13.3565(10), *b* 7.8477(5), *c* 14.7075(12) Å, α 111.535(14), β 94.311(13), γ 101.586(12)°, *V* 1416.4(2) Å³, space group P1̄, *Z* 2, $\mu(\text{Mo K}\alpha)$ 0.125 mm^{−1}, 288 refinement parameters, 3662 reflections measured, 1504 unique (*R*_{int} = 0.0711) which were used in all calculations. CCDC 2,225,829 contains the supplementary crystallographic data for this compound.

The main crystallographic data for **23**: C₁₉H₁₂F₂N₂O₃, *M* 354.31, monoclinic, *a* 14.0716(10), *b* 7.7151(5), *c* 14.5964(12) Å, β 100.453(7)°, *V* 1553.0(2) Å³, space group P2₁/c, *Z* 4, $\mu(\text{Mo K}\alpha)$ 0.125 mm^{−1}, 257 refinement parameters, 4236 reflections measured, and 2349 unique (*R*_{int} = 0.0568) which were used in all calculations. CCDC 2,225,830 contains the supplementary crystallographic data for this compound.

3.4. Fungistatic Activity Evaluation

The following dermatophyte fungal strains were used: *Trichophyton rubrum* (RCPF F 1408), *Epidermophyton floccosum* (RCPF F 1659/17), and *Microsporum canis* (RCPF F 1643/1585), as well as yeast-like fungus *Candida parapsilosis* (RCPF 1245/ ATCC 22019). The fungi cultures were obtained from the Russian Collection of Pathogenic Fungi (Kashkin Research Institute of Medical Mycology; Mechnikov Northwest State Medical University, St.-Petersburg). Saburo agar and Saburo broth were used for the fungi. The microorganisms were identified as matrix-extracted bacterial proteins with an accuracy of 99.9% using a BioMerieux VITEK MS MALDI-TOF analyzer. The test cultures were prepared to an optical density of 0.5 according to McFarland (1.5 × 10⁸ CFU/ mL) using a BioMerieux DensiCHEK densimeter. The suspensions of *C. parapsilosis* were prepared from 24 h cultures, and dermatophyte inocula were prepared after incubation for 2 weeks and preliminary homogenization in sterile saline. The fungi were inoculated at a concentration of 10⁵ CFU/mL.

The antimycotic activity was evaluated by a micro method [54]. The agar nutrient medium was maintained in liquid by heating to 52 °C. The chemical compounds to be tested were dissolved in DMSO to a concentration of 1000 µg/ mL, and the stock solutions were diluted with distilled sterilized water; serial dilutions (from 250–200 µg/ mL) were made using nutrient media. Dermatophytes were incubated at 27 °C for up to 7–10 days and *C. parapsilosis* for 24 h in a moist 5.0% CO₂ chamber. In each case, positive and negative controls were used. The minimum inhibitory concentration was determined visually as the lowest concentration at which a test culture no longer grows. Chemically pure fluconazole was used as a reference drug.

4. Conclusions

The data obtained in this work and earlier in the study of transformations with pyrazole [29] thus indicate that base-promoted reactions of nucleophilic aromatic substitution are a convenient method for the functionalization of polyfluoroflavones 1–3 with azoles with different numbers of nitrogen atoms. At the same time, it was found that monosubstitution of the para-fluorine atom successfully and selectively occurs while using the system (azole (1.5 equiv.)/NaOBu^t (1.5 equiv.)/MeCN) regardless of the structure and properties of the used polyfluorinated substrates and nucleophilic reagents, since in all cases, mono(azolyl)-substituted flavones were obtained in good yields. Under the conditions (azole (6 equiv.)/NaOBu^t (6 equiv.)/DMF), which promote the formation of persubstituted products, the interactions of polyfluoroflavones 1–3 with pyrazole are distinguished by high selectivity [26], while similar reactions with triazole produced productively only for penta- and tetrafluoroflavones 1 and 2, and the same transformations with imidazole in general are extremely non-selective.

Comparing the conversion of polyfluoroflavones 1–3 in reactions with azoles under conditions that do not provide selective substitution (azole (3 equiv.)/Cs₂CO₃ (3 equiv.)/MeCN)), it can be noted that transformations with pyrazole [26] are characterized by easier formation of polysubstituted products, and under conditions conducive to persubstitution, it is possible to build the following series of azoles according to reactivity: pyrazole ≥ triazole > imidazole. Obviously, in both cases, the reactivity of azoles does not correspond to their basicity, and therefore to some extent, nucleophilicity, since imidazole is known to be the strongest base among them [55]. According to the literature data [56,57], polyfluoroaromatic compounds generally react with nucleophiles via Meisenheimer complexes. For flavones 1–3, we assume an analogous mechanism [26]; first nucleophile attack occurs on the activated C4' site of flavones 1–3 with the generation of an intermediate of a stable quinoid structure, followed by formation of a mono(azolyl)-substituted product. Sequential substitution is coordinated by the joint activating effect of the substituents, and the resulting intermediate complexes are stabilized both by O,N-bidentate coordination between the azole and the pyrone fragment of the molecule with Na⁺ and by the coordination of neighboring azole moieties with Na⁺. It is likely that the higher reactivity of pyrazole, triazole, and their intermediates compared to imidazole and its derivatives in S_NAr poly- and per-substitution reactions is due to the possibility of participation of their imine nitrogen atoms in the N–N=C function in coordination during the formation of transitional complexes.

In addition, it was shown that the per-substitution conditions can be successfully used for the synthesis of polynuclear hybrid compounds containing two different azole fragments by the reaction of mono(azolyl)-substituted flavones with pyrazole and triazole.

Using XRD data, the structural features of triazolyl- and imidazolyl-substituted flavones in crystal form were established. For example, in contrast to previously synthesized pyrazole analogues [26], new azole derivatives do not contain an intramolecular H-bond.

In terms of possible practical applications, it has been established that the resulting poly(pyrazolyl)-substituted flavones have luminescent properties, which makes further

development of research in this area promising. In addition, weak antimycotic activity was found for some azolyl-containing flavones.

Supplementary Materials: NMR data of the synthesized compounds can be downloaded at: <https://www.mdpi.com/article/10.3390/molecules28020869/s1>. Figure S1. ^1H NMR spectrum of compound 4; Figure S2. ^{13}C NMR spectrum of compound 4; Figure S3. ^{19}F NMR spectrum of compound 4; Figure S4. ^1H NMR spectrum of compound 7; Figure S5. ^{13}C NMR spectrum of compound 7; Figure S6. ^1H NMR spectrum of compound 8; Figure S7. ^{13}C NMR spectrum of compound 8; Figure S8. ^{19}F NMR spectrum of compound 8; Figure S9. ^1H NMR spectrum of compound 9; Figure S10. ^{19}F NMR spectrum of compound 9; Figure S11. ^1H NMR spectrum of compound 10; Figure S12. ^{13}C NMR spectrum of compound 10; Figure S13. ^{19}F NMR spectrum of compound 10; Figure S14. ^1H NMR spectrum of compound 11; Figure S15. ^{13}C NMR spectrum of compound 11; Figure S16. ^{19}F NMR spectrum of compound 11; Figure S17. ^1H NMR spectrum of compound 14; Figure S18. ^{13}C NMR spectrum of compound 14; Figure S19. ^1H NMR spectrum of compound 15; Figure S20. ^{13}C NMR spectrum of compound 15; Figure S21. ^{19}F NMR spectrum of compound 15; Figure S22. ^1H NMR spectrum of compound 17; Figure S23. ^{13}C NMR spectrum of compound 17; Figure S24. ^{19}F NMR spectrum of compound 17; Figure S25. ^1H NMR spectrum of compound 18; Figure S26. ^{13}C NMR spectrum of compound 18; Figure S27. ^{19}F NMR spectrum of compound 18; Figure S28. ^1H NMR spectrum of compound 19; Figure S29. ^{13}C NMR spectrum of compound 19; Figure S30. ^{19}F NMR spectrum of compound 19; Figure S31. ^1H NMR spectrum of compound 22; Figure S32. ^{13}C NMR spectrum of compound 22; Figure S33. ^{19}F NMR spectrum of compound 22; Figure S34. ^1H NMR spectrum of compound 23; Figure S35. ^{13}C NMR spectrum of compound 23; Figure S36. ^{19}F NMR spectrum of compound 23; Figure S37. ^1H NMR spectrum of compound 26; Figure S38. ^{13}C NMR spectrum of compound 26; Figure S39. ^{19}F NMR spectrum of compound 26; Figure S40. ^1H NMR spectrum of compound 27; Figure S41. ^{13}C NMR spectrum of compound 27; Figure S42. ^1H NMR spectrum of compound 28; Figure S43. ^{13}C NMR spectrum of compound 28; Figure S44. ^1H NMR spectrum of compound 29; Figure S45. ^{13}C NMR spectrum of compound 29; Figure S46. ^1H NMR spectrum of compound 31; Figure S47. ^{13}C NMR spectrum of compound 31.

Author Contributions: Conceptualization Y.V.B.; methodology and synthesis, validation, and interpretation of analysis data, K.V.S. and M.A.P.; analytical experiments E.F.Z.; writing—original draft preparation, K.V.S. and M.A.P.; writing—review and editing, Y.V.B.; supervision, V.I.S. All authors have read and agreed to the published version of the manuscript.

Funding: This work was financially supported by the Ministry of Science and Higher Education of the Russian Federation (State task AAAA-A19-119012290115-2).

Institutional Review Board Statement: Not applicable.

Informed Consent Statement: Not applicable.

Data Availability Statement: Not applicable.

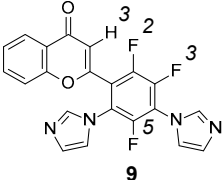
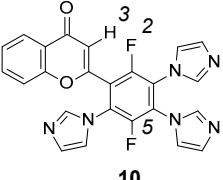
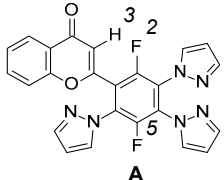
Acknowledgments: The analytical data analysis (IR and NMR spectroscopy, elemental analysis, XRD analysis, and photoluminescent data) was performed on equipment belonging to the Center for Joint Use of Scientific Equipment “Spectroscopy and Analysis of Organic Compounds” IOS UB RAS. Fungistatic activity evaluation was performed on equipment belonging to the Ural Research Institute of Dermatovenereology and Immunopathology, Yekaterinburg, Russian Federation. The authors acknowledge Natalia A. Gerasimova for her contribution.

Conflicts of Interest: The authors declare no conflict of interest.

Sample Availability: Samples of the compounds are available from the authors.

Appendix A

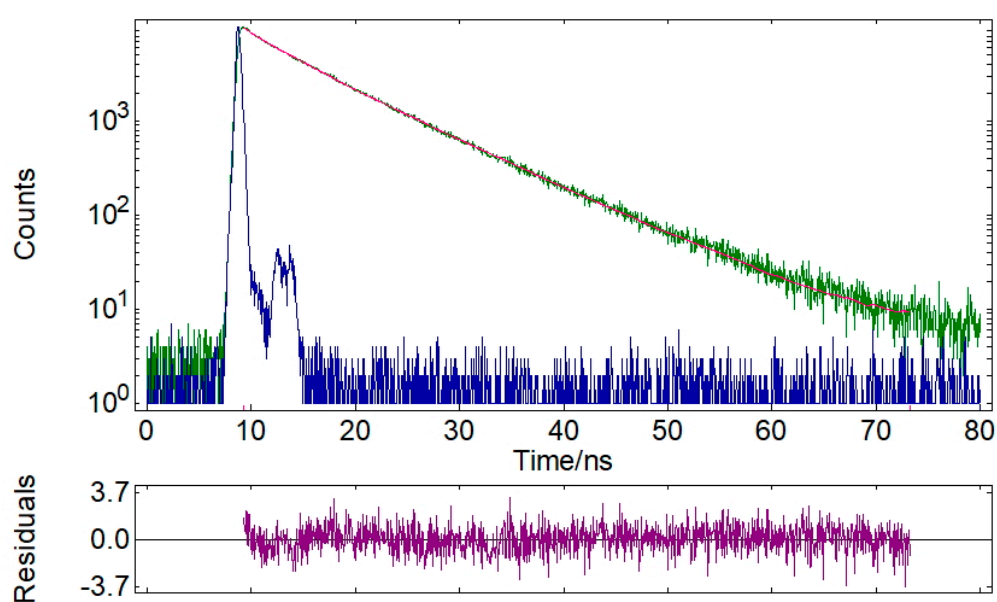
Table A1. NMR data of characteristic F and H nuclei of flavones 9, 10, and A.

Compound	H3		F2		F3		F5	
	δ	J	δ	J	δ	J	δ	J
<div style="text-align: center;">  9 </div>	6.52, d	$^5J_{\text{HF}}$ 1.4	26.33 ddd	$^3J_{\text{FF}}$ 22.6 $^5J_{\text{FF}}$ 13.0 $^5J_{\text{FH}}$ 1.4	23.60 d	$^3J_{\text{FF}}$ 22.4	30.57 d	$^5J_{\text{FF}}$ 13.1
<div style="text-align: center;">  10 </div>	6.51, d	$^5J_{\text{HF}}$ 1.3	41.18 dd	$^5J_{\text{FF}}$ 14.7 $^5J_{\text{FH}}$ 1.3	—	—	31.47 d	$^5J_{\text{FF}}$ 14.7
<div style="text-align: center;">  A </div>	6.44, d	$^5J_{\text{HF}}$ 1.1	29.51 dd	$^5J_{\text{FF}}$ 14.4 $^5J_{\text{FH}}$ 1.1	—	—	39.83 d	$^5J_{\text{FF}}$ 14.3

Appendix B

Table A2. Detailed data of the fluorescence lifetime measurements of 28 and 32: τ —lifetime, f —fractional contribution, τ_{avg} —average lifetime, and χ^2 —chi-squared distribution.

Compound	Solid					
	τ_1 , ns	f_1 , %	τ_2 , ns	f_2 , %	τ_{avg} , ns	χ^2
28	3.57	16.5	8.53	83.5	7.72	1.109
32	2.84	21.3	7.88	78.7	6.81	1.206

Figure A1. Time-resolved fluorescence lifetime decay profile of solid powder 28 (green) and instrumental response function (IRF, blue). λ_{ex} = 375 nm and λ_{em} = 504 nm.

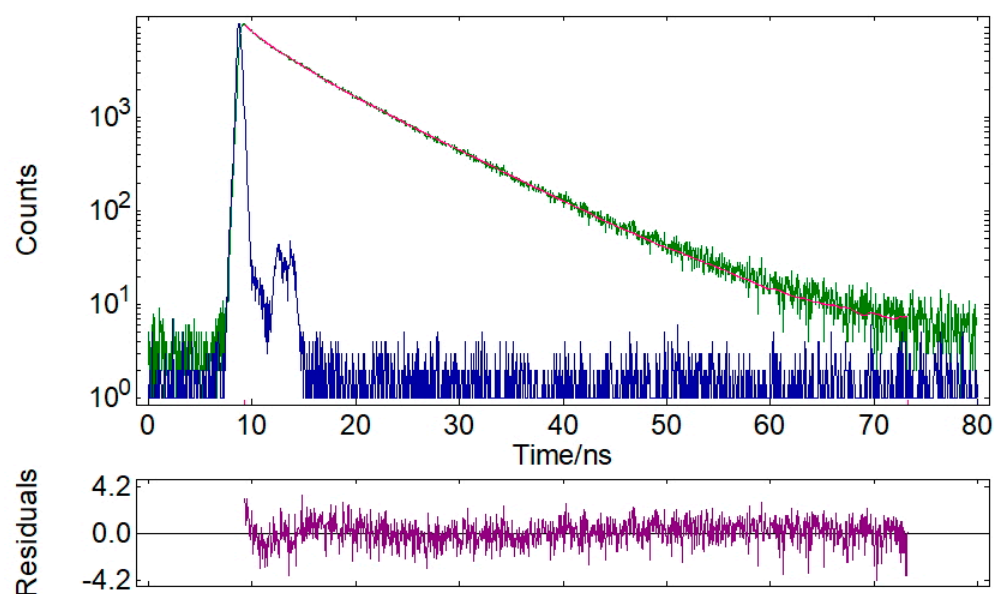


Figure A2. Time-resolved fluorescence lifetime decay profile of solid powder **32** (green), instrumental response function (IRF, blue). $\lambda_{\text{ex}} = 375$ nm and $\lambda_{\text{em}} = 504$ nm.

Appendix C

Table A3. Fungistatic activity of fluorinated flavones and their azolyl-substituted derivatives.

No	Compounds					MIC ($\mu\text{g/mL}$)/MIC ₅₀ ($\mu\text{g/mL}$)			
	R ¹	R ²	R ³	R ⁴	R ⁵	<i>T. rubrum</i>	<i>E. floccosum</i>	<i>M. canis</i>	<i>C. parapsilosis</i>
4	F	F	trz	F	F	>200	>200	>200	>200
8	F	F	imz	F	F	100/25	200/100	100/50	>200
11	H	F	trz	F	F	>200	>200	>200	>200
14	H	trz	trz	trz	trz	100/25	200/100	100/50	>200
18	OMe	F	trz	F	H	>200	>200	>200	>200
19	OMe	trz	trz	F	H	-	>200/50	>200/200	>200/200
23	OMe	F	imz	F	H	>200/12.5	>200/12.5	>200/6.25	>200
26	F	pz	trz	F	pz	>200	>200	>200	>200
33	OMe	pz	pz	F	H	>100/1.56	>100/1.56	>100	>100
34	F	pz	pz	F	pz	>100	>100	>100	>100
35	pz	pz	pz	pz	pz	>100	>100	>100	>100
Fluconazole						3.12	1.56	3.12	0.5–2

References

1. Tian, S.; Luo, T.; Zhu, Y.; Wan, J.-P. Recent advances in diversification of chromones and flavones by direct C–H bond activation or functionalization. *Chin. Chem. Lett.* **2020**, *31*, 3073–3082. [[CrossRef](#)]

2. Kshatriya, R.; Jejurkar, V.P.; Saha, S. Recent advances in the synthetic methodologies of flavones. *Tetrahedron* **2018**, *74*, 811–833. [\[CrossRef\]](#)
3. Spagnuolo, C.; Moccia, S.; Russo, G.L. Anti-inflammatory effects of flavonoids in neurodegenerative disorders. *Eur. J. Med. Chem.* **2018**, *153*, 105–115. [\[CrossRef\]](#)
4. Singh, M.; Kaur, M.; Silakari, O. Flavones: An important scaffold for medicinal chemistry. *Eur. J. Med. Chem.* **2014**, *84*, 206–239. [\[CrossRef\]](#) [\[PubMed\]](#)
5. Verma, A.K.; Singh, H.; Satyanarayana, M.; Srivastava, S.P.; Tiwari, P.; Singh, A.B.; Dwivedi, A.K.; Singh, S.K.; Srivastava, M.; Nath, C.; et al. Flavone-based novel antidiabetic and antidyslipidemic agents. *J. Med. Chem.* **2012**, *55*, 4551–4567. [\[CrossRef\]](#) [\[PubMed\]](#)
6. Lo, M.-M.; Benfodda, Z.; Dunyach-Rémy, C.; Béniméris, D.; Roulard, R.; Fontaine, J.-X.; Mathiron, D.; Quéro, A.; Molinié, R.; Meffre, P. Isolation and identification of flavones responsible for the antibacterial activities of *Tillandsia bergeri* extracts. *ACS Omega* **2022**, *7*, 35851–35862. [\[CrossRef\]](#) [\[PubMed\]](#)
7. Dong, H.; Wu, M.; Xiang, S.; Song, T.; Li, Y.; Long, B.; Feng, C.; Shi, Z. Total syntheses and antibacterial evaluations of neocyclomorusin and related flavones. *J. Nat. Prod.* **2022**, *85*, 2217–2225. [\[CrossRef\]](#) [\[PubMed\]](#)
8. Rubin, D.; Sansom, C.E.; Lucas, N.T.; McAdam, J.C.; Simpson, J.; Lord, J.M.; Perry, N.B. O-Acylated flavones in the alpine daisy *Celmisia viscosa*: Intraspecific variation. *J. Nat. Prod.* **2022**, *85*, 1904–1911. [\[CrossRef\]](#) [\[PubMed\]](#)
9. Wang, X.; Cao, Y.; Chen, S.; Lin, J.; Yang, X.; Huang, D. Structure–activity relationship (SAR) of flavones on their anti-inflammatory activity in murine macrophages in culture through the NF- κ B pathway and c-Src kinase receptor. *J. Agric. Food Chem.* **2022**, *70*, 8788–8798. [\[CrossRef\]](#) [\[PubMed\]](#)
10. Tsai, H.-Y.; Chen, M.-Y.; Hsu, C.; Kuan, K.-Y.; Chang, C.-F.; Wang, C.-W.; Hsu, C.-P.; Su, N.-W. Luteolin phosphate derivatives generated by cultivating *Bacillus subtilis* var. Natto BCRC 80517 with luteolin. *J. Agric. Food Chem.* **2022**, *70*, 8738–8745. [\[CrossRef\]](#) [\[PubMed\]](#)
11. Dong, H.; Wu, M.; Li, Y.; Lu, L.; Qin, J.; He, Y.; Shi, Z. Total syntheses and anti-inflammatory evaluations of pongamosides A–C, natural furanoflavonoid glucosides from fruit of *Pongamia pinnata* (L.) Pierre. *J. Nat. Prod.* **2022**, *85*, 1118–1127. [\[CrossRef\]](#)
12. Li, J.; Tan, L.-H.; Zou, H.; Zou, Z.-X.; Long, H.-P.; Wang, W.-X.; Xu, P.-S.; Liu, L.-F.; Xu, K.-P.; Tan, G.-S. Palhinisides A–H: Flavone glucosidic truxinate esters with neuroprotective activities from *Palhinhaea cernua*. *J. Nat. Prod.* **2020**, *83*, 216–222. [\[CrossRef\]](#) [\[PubMed\]](#)
13. Lin, S.; Koh, J.-J.; Aung, T.T.; Sin, W.L.W.; Lim, F.; Wang, L.; Lakshminarayanan, R.; Zhou, L.; Tan, D.T.H.; Cao, D.; et al. Semisynthetic flavone-derived antimicrobials with therapeutic potential against methicillin-resistant *Staphylococcus aureus* (MRSA). *J. Med. Chem.* **2017**, *60*, 6152–6165. [\[CrossRef\]](#)
14. Pajtás, D.; Kónya, K.; Kiss-Szikszai, A.; Džubák, P.; Pethő, Z.; Varga, Z.; Panyi, G.; Patonay, T. Optimization of the synthesis of flavone–amino acid and flavone–dipeptide hybrids via Buchwald–Hartwig reaction. *J. Org. Chem.* **2017**, *82*, 4578–4587. [\[CrossRef\]](#) [\[PubMed\]](#)
15. Byun, Y.; Moon, K.; Park, J.; Ghosh, P.; Mishra, N.K.; Kim, I.S. Methylene thiazolidinediones as alkylation reagents in catalytic C–H functionalization: Rapid access to glitazones. *Org. Lett.* **2022**, *24*, 8578–8583. [\[CrossRef\]](#) [\[PubMed\]](#)
16. Xiong, Y.; Schaus, S.E.; Porco, J.A., Jr. Metal-catalyzed cascade rearrangements of 3-alkynyl flavone ethers. *Org. Lett.* **2013**, *15*, 1962–1965. [\[CrossRef\]](#)
17. Hosseini, S.; Thapa, B.; Medeiros, M.J.; Pasciak, E.M.; Pence, M.A.; Twum, E.B.; Karty, J.A.; Gao, X.; Raghavachari, K.; Peters, D.G.; et al. Electrosynthesis of a baurone by controlled dimerization of flavone: Mechanistic insight and large-scale application. *J. Org. Chem.* **2020**, *85*, 10658–10669. [\[CrossRef\]](#)
18. Tang, Q.; Bian, Z.; Wu, W.; Wang, J.; Xie, P.; Pittman, C.U., Jr.; Zhou, A. Making flavone thi-oethers using halides and powdered sulfur or Na₂S₂O₃. *J. Org. Chem.* **2017**, *82*, 10617–10622. [\[CrossRef\]](#)
19. Tokárová, Z.; Balogh, R.; Tisovský, P.; Hrnčariková, K.; Végh, D. Direct nucleophilic substitution of polyfluorobenzenes with pyrrole and 2,5-dimethylpyrrole. *J. Fluorine Chem.* **2017**, *204*, 59–64. [\[CrossRef\]](#)
20. Gerencsér, J.; Balázs, A.; Dormán, G. Synthesis and modification of heterocycles by metal-catalyzed cross-coupling reactions. In *Topics in Heterocyclic Chemistry*; Patonay, T., Kónya, K., Eds.; Springer International Publishing AG: Cham, Switzerland, 2016; Volume 45.
21. Kong, X.; Zhang, H.; Cao, C.; Shi, Y.; Pang, G. Effective transition metal free and selective C–F activation under mild conditions. *RSC Adv.* **2015**, *5*, 7035–7048. [\[CrossRef\]](#)
22. Boelke, A.; Sadat, S.; Lork, E.; Nachtsheim, B.J. Pseudocyclic bis-N-heterocycle-stabilized iodanes—Synthesis, characterization and applications. *Chem. Commun.* **2021**, *57*, 7434–7437. [\[CrossRef\]](#) [\[PubMed\]](#)
23. Zhong, W.; Wang, L.; Qin, D.; Zhou, J.; Duan, H. Two novel fluorescent probes as systematic sensors for multiple metal ions: Focus on detection of Hg²⁺. *ACS Omega* **2020**, *5*, 24285–24295. [\[CrossRef\]](#) [\[PubMed\]](#)
24. Zhou, Q.; Hong, X.; Cui, H.-Z.; Huang, S.; Yi, Y.; Hou, X.-F. The construction of C–N, C–O, and C(sp²)–C(sp³) bonds from fluorine-substituted 2-aryl benzazoles for direct synthesis of N-, O-, C-functionalized 2-aryl benzazole derivatives. *J. Org. Chem.* **2018**, *83*, 6363–6372. [\[CrossRef\]](#) [\[PubMed\]](#)
25. Santos, C.M.M.; Silva, V.L.M.; Silva, A.M.S. Synthesis of chromone-related pyrazole compounds. *Molecules* **2017**, *22*, 1665–1713. [\[CrossRef\]](#) [\[PubMed\]](#)

26. Shcherbakov, K.V.; Panova, M.A.; Burgart, Y.V.; Saloutin, V.I. Selective nucleophilic aromatic substitution of 2-(polyfluorophenyl)-4H-chromen-4-ones with pyrazole. *J. Fluorine Chem.* **2022**, *263*, 110034. [\[CrossRef\]](#)
27. Shcherbakov, K.V.; Artemyeva, M.A.; Burgart, Y.V.; Saloutin, V.I.; Volobueva, A.S.; Misiurina, M.A.; Esaulkova, Y.L.; Sinegubova, E.O.; Zarubaev, V.V. 7-Imidazolylsubstituted 4'-methoxy and 3',4'-dimethoxy-containing polyfluoroflavones as promising antiviral agents. *J. Fluorine Chem.* **2020**, *240*, 109657. [\[CrossRef\]](#)
28. Podlech, J. Elimination of fluorine to form C–N bonds. In *Organo-Fluorine Compounds*, 4th ed.; Baasner, B., Hagemann, H., Tatlow, J.C., Eds.; Georg Thieme Verlag: Stuttgart, Germany, 1999; pp. 449–464.
29. Shcherbakov, K.V.; Panova, M.A.; Burgart, Y.V.; Zarubaev, V.V.; Gerasimova, N.A.; Evstigneeva, N.P.; Saloutin, V.I. The synthesis and biological evaluation of A- and B-ring fluorinated flavones and their key intermediates. *J. Fluorine Chem.* **2021**, *249*, 109857. [\[CrossRef\]](#)
30. Shcherbakov, K.V.; Artemyeva, M.A.; Burgart, Y.V.; Evstigneeva, N.P.; Gerasimova, N.A.; Zilberberg, N.V.; Kungurov, N.V.; Saloutin, V.I.; Chupakhin, O.N. Transformations of 3-acyl-4H-polyfluorochromen-4-ones under the action of amino acids and biogenic amines. *J. Fluorine Chem.* **2019**, *226*, 109354. [\[CrossRef\]](#)
31. Shcherbakov, K.V.; Burgart, Y.V.; Saloutin, V.I.; Chupakhin, O.N. Modification of polyfluoro-containing 3-(ethoxycarbonyl)flavones by biogenic amines and amino acids. *Curr. Org. Synth.* **2018**, *15*, 707–714. [\[CrossRef\]](#)
32. Shcherbakov, K.V.; Burgart, Y.V.; Saloutin, V.I.; Chupakhin, O.N. Polyfluorinecontaining chromen-4-ones: Synthesis and transformations. *Russ. Chem. Bull.* **2016**, *65*, 2151–2162. [\[CrossRef\]](#)
33. Ahmadi, A.; Mohammadnejadi, E.; Karami, P.; Razzaghi-Asi, N. Current status and structure activity relationship of privileged azoles as antifungal agents. *Int. J. Antimicrob. Agents* **2022**, *59*, 106518. [\[CrossRef\]](#)
34. Seck, I.; Nguemo, F. Triazole, imidazole, and thiazole-based compounds as potential agents against coronavirus. *Results Chem.* **2021**, *3*, 100132. [\[CrossRef\]](#)
35. Kerru, N.; Gummidi, L.; Maddila, S.; Gangu, K.K.; Jonnalagadda, S.B. A review on recent advances in nitrogen-containing molecules and their biological applications. *Molecules* **2020**, *25*, 1909–1951. [\[CrossRef\]](#) [\[PubMed\]](#)
36. Aggarwal, R.; Sumran, G. An insight on medicinal attributes of 1,2,4-triazoles. *Eur. J. Med. Chem.* **2020**, *205*, 112652. [\[CrossRef\]](#) [\[PubMed\]](#)
37. Prasher, P.; Sharma, M. “Azole” as privileged heterocycle for targeting the inducible cyclooxygenase enzyme. *Drug Dev. Res.* **2020**, *82*, 167–197. [\[CrossRef\]](#)
38. Hou, Y.; Shang, C.; Wang, H.; Yun, J. Isatin-azole hybrids and their anticancer activities. *Arch. Pharm. Chem. Life Sci.* **2019**, *353*, e1900272. [\[CrossRef\]](#) [\[PubMed\]](#)
39. Xu, M.; Peng, Y.; Wang, S.; Ji, J.; Rakesh, K.P. Triazole derivatives as inhibitors of Alzheimer’s disease: Current developments and structure-activity relationships. *Eur. J. Med. Chem.* **2019**, *180*, 656–672. [\[CrossRef\]](#) [\[PubMed\]](#)
40. Fan, Y.-L.; Jin, X.-H.; Huang, Z.-P.; Yu, H.-F.; Zeng, Z.-G.; Gao, T.; Feng, L.-S. Recent advances of imidazole-containing derivatives as anti-tubercular agents. *Eur. J. Med. Chem.* **2018**, *150*, 347–365. [\[CrossRef\]](#)
41. Yan, M.; Xu, L.; Wang, Y.; Wan, J.; Liu, T.; Liu, W.; Wan, Y.; Zhang, B.; Wang, R. Opportunities and challenges of using five-membered ring compounds as promising antitubercular agents. *Drug Dev. Res.* **2020**, *81*, 402–418. [\[CrossRef\]](#)
42. Gao, F.; Wang, T.; Xiao, J.; Huang, G. Antibacterial activity study of 1,2,4-triazole derivatives. *Eur. J. Med. Chem.* **2019**, *173*, 274–281. [\[CrossRef\]](#)
43. Teli, G.; Chawla, P.A. Hybridization of imidazole with various heterocycles in targeting cancer. *ChemistrySelect* **2021**, *6*, 4803–4836. [\[CrossRef\]](#)
44. Zhang, J.; Wang, S.; Ba, Y.; Xu, Z. 1,2,4-Triazole-quinoline/quinolone hybrids as potential anti-bacterial agents. *Eur. J. Med. Chem.* **2019**, *174*, 1–8. [\[CrossRef\]](#)
45. Fan, Y.-L.; Liu, M. Coumarin-triazole hybrids and their biological activities. *J. Heterocycl. Chem.* **2018**, *55*, 791–802. [\[CrossRef\]](#)
46. Zhang, T.; Zhu, M.; Li, J.; Zhang, Y.; Wang, X. Bipolar host materials comprising carbazole, pyridine and triazole moieties for efficient and stable phosphorescent OLEDs. *Dyes Pigm.* **2021**, *192*, 109426. [\[CrossRef\]](#)
47. Ye, S.; Zhuang, S.; Pan, B.; Guo, R.; Wang, L. Imidazole derivatives for efficient organic light-emitting diodes. *J. Inf. Disp.* **2020**, *21*, 173–196. [\[CrossRef\]](#)
48. Xu, H.; Zhao, Y.; Zhang, J.; Zhang, D.; Miao, Y.; Shinar, J.; Shinar, R.; Wang, H.; Xu, B. Low efficiency rol-off phosphorescent organic light-emitting devices using thermally activated delayed fluorescence hosts materials based 1,2,4-triazole acceptor. *Org. Electron.* **2019**, *74*, 13–22. [\[CrossRef\]](#)
49. Tao, Y.; Yang, C.; Qin, J. Organic host materials for phosphorescent organic light-emitting diodes. *Chem. Soc. Rev.* **2011**, *40*, 2943–2970. [\[CrossRef\]](#)
50. Emami, L.; Faghih, Z.; Ataollahi, E. Azole derivatives: Recent advances as potent antibacterial and antifungal agents. *Curr. Med. Chem.* **2022**, *129*, 220–249. [\[CrossRef\]](#)
51. Dolomanov, O.V.; Bourhis, L.J.; Gildea, R.J.; Howard, J.A.K.; Puschmann, H. OLEX2: A complete structure solution, refinement and analysis program. *J. Appl. Crystallogr.* **2009**, *42*, 339–341. [\[CrossRef\]](#)
52. Palatinus, L.; Chapuis, G. SUPERFLIP—A computer program for the solution of crystal structures by charge flipping in arbitrary dimensions. *J. Appl. Crystallogr.* **2007**, *40*, 786–790. [\[CrossRef\]](#)
53. Sheldrick, G.M. A short history of SHELX. *Acta Crystallogr. Sect. A Found. Crystallogr.* **2007**, *64*, 112–122. [\[CrossRef\]](#) [\[PubMed\]](#)

54. Kubanova, A.A.; Stepanova, Z.V.; Gus'kova, T.A.; Pushkina, T.V.; Krylova, L.Y.; Shilova, I.B.; Trenin, A.S. Metodicheskie rekomendacii po izucheniyu protivogribkovoï aktivnosti lekarstvennykh sredstv (Guidelines for the study of the antifungal activity of medicines). In *Rukovodstvo po Provedeniyu Doklinicheskikh Issledovaniï Lekarstvennykh Sredstv (A Guide to Preclinical Trials of Medicines)*; Mironov, A.N., Ed.; Grif i K: Moscow, Russia, 2012; pp. 578–586.
55. Koldobskii, G.I.; Ostrovskii, V.A. Acid-base properties of five-membered nitrogen-containing heterocycles. *Chem. Heterocycl. Compds.* **1988**, *24*, 469–480. [[CrossRef](#)]
56. Krishnan, R.; Parthiban, A. Regioselective preparation of functional aryl ethers and esters by stepwise nucleophilic aromatic substitution reaction. *J. Fluorine Chem.* **2014**, *162*, 17–25. [[CrossRef](#)]
57. Chambers, R.D.; Martin, P.A.; Sandford, G.; Williams, L.H. Mechanisms of reactions of halogenated compounds: Part 7. Effects of fluorine and other groups as substituents on nucleophilic aromatic substitution. *J. Fluorine Chem.* **2008**, *129*, 998–1002. [[CrossRef](#)]

Disclaimer/Publisher's Note: The statements, opinions and data contained in all publications are solely those of the individual author(s) and contributor(s) and not of MDPI and/or the editor(s). MDPI and/or the editor(s) disclaim responsibility for any injury to people or property resulting from any ideas, methods, instructions or products referred to in the content.